KANSAS GEOLOGICAL SURVEY
OPEN-FILE REPORT 98-64

Sequence Stratigraphy of the Lane-Island Creek Shales and the Farley Limestone, Kansas City Area, NE Kansas

by

J. McKirahan
R.H. Goldstein
E.K. Franseen

Kansas Geological Survey
1930 Constant Avenue
University of Kansas
Lawrence, KS 66047-3726

Sequence Stratigraphy of the Lane-Island Creek Shales and the Farley Limestone, Kansas City Area, NE Kansas

By

J. McKirahan[1], R.H. Goldstein[1] & E.K. Franseen[2]

[1]University of Kansas, Department of Geology, Lawrence, KS 66045

[2]University of Kansas, Kansas Geological Survey, Lawrence, KS 66047

Kansas Geological Survey Open-File Report 98-64

Introduction

Historically, Pennsylvanian carbonate units of Kansas such as the Farley Limestone generally have been thought of as continuous layers. Upon close inspection, however, they reveal significant lateral and vertical variability of facies and geometry. The objective of this paper is to describe the stratigraphy and sedimentology of the Farley Limestone in northeastern Kansas with emphasis on evaluating the controls of the lateral and vertical distribution of both facies and stratal geometries. We hypothesize that the Farley was affected by depositional topography, source and distribution of siliciclastics, and changes in relative sea level. The development of a high-resolution sequence-stratigraphic framework for the Farley Limestone allows better understanding of how these factors controlled heterogeneity of facies.

A firm understanding of the sequence-stratigraphic framework of a unit such as the Farley Limestone provides a better understanding of the interaction of factors that control lithologic heterogeneity and provides predictive capabilities that are applicable to other Pennsylvanian limestone units similar to the Farley. Because many Pennsylvanian carbonate units similar to the Farley are petroleum reservoirs, these predictive capabilities are potentially useful for locating potential petroleum reservoirs in addition to identification of high-quality limestone aggregate resources.

Area of Study

The field area in this study includes a combination of 18 quarry exposures, roadcuts, and drill cores in Johnson, Wyandotte, and Leavenworth counties in the Kansas City area of northeastern Kansas (Figure 1).

Stratigraphy

Described first in Missouri by Hinds and Green (1915), the Farley Limestone was defined as a thin limestone lying between the Argentine and Plattsburg Limestones

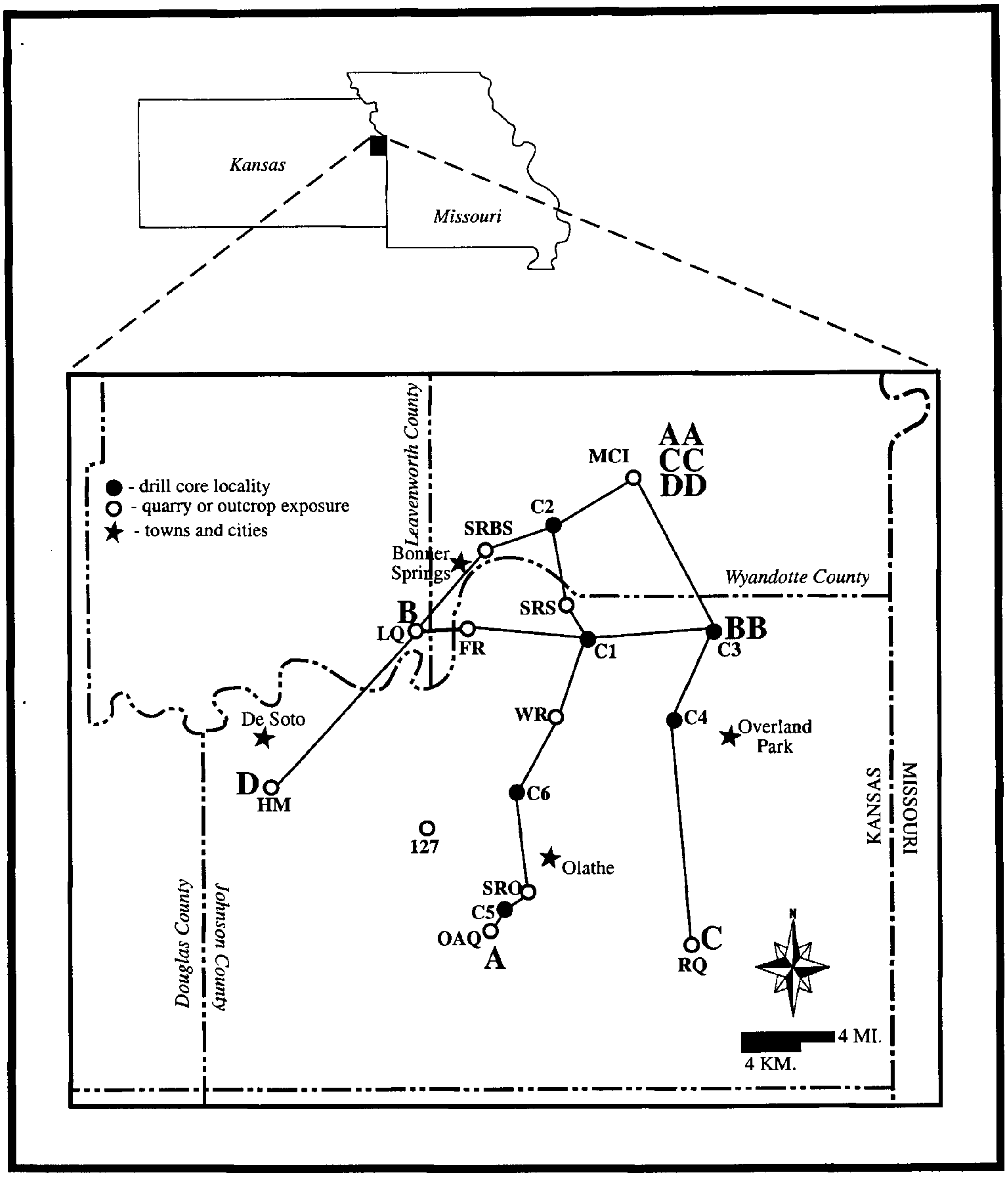

Figure.1: Index map showing location and type of field localaties and major towns for reference. Reconstructed cross-sections along lines A-AA, B-BB, C-CC, and D-DD are illustrated in Figures 2.30, 2.31, 2.32, and 2.33.

and was placed as the middle member of the Lane Shale (Watney and Heckel, 1994). Moore (1932) and Newell (1935) later identified the Farley in northeastern Kansas (Johnson County) as two lithologically similar limestones separated by a shale unit and placed it as the upper member of the Wyandotte Limestone. Still later, Moore (1949) showed that in Kansas, north of Miami County, the Farley occurs as an extremely variable assemblage of limestone and shale beds above the more laterally persistent Argentine Limestone.

The stratigraphic nomenclature presented in this paper (Figure 2A) reflects recent changes made by Arvidson (1990) and Watney and Heckel (1994), to the traditional stratigraphic classification (Figure 2B). The new stratigraphic nomenclature corrects a miscorrelation made by Moore (1935) who placed the Lane Shale below the Argentine Limestone rather than above it. The Farley is located above one of three different units depending on location within the field area. In the north and northeast the Farley is located immediately above the Island Creek Shale. In the southwest it overlies the Lane Shale and in the areas where these shale units are absent the Farley is found directly overlying the Argentine Limestone. The unit located directly over the Farley Limestone in all localities is the Bonner Springs Shale. A brief introduction to each of these units is presented below.

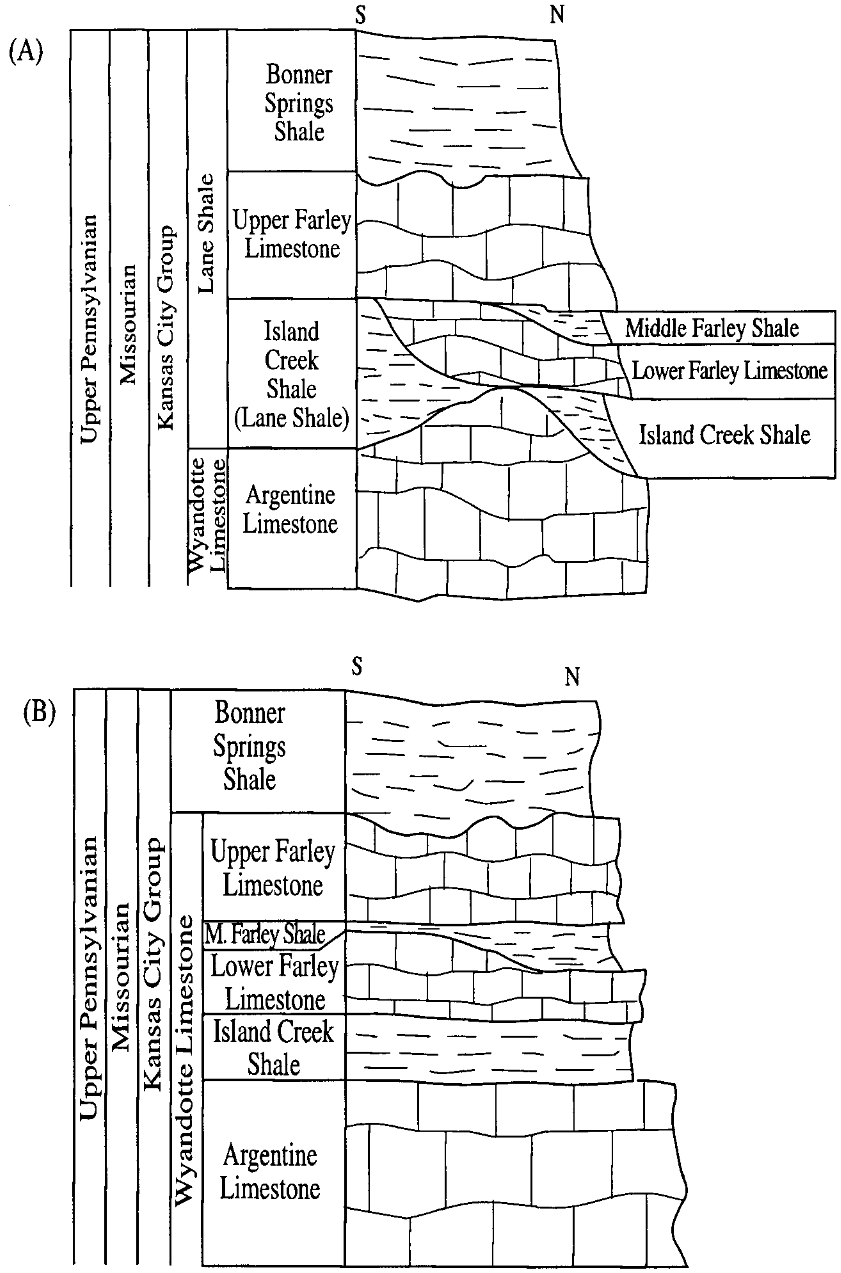

Figure 2. Generalized stratigraphic sections showing general relationships and lithologies of the units examined for this study. (A) Section showing revised stratigraphic nomenclature based on the work of Arvidson (1990) and Watney & Heckel, (1994). Major revisions include splitting the Farley Limestone and the Bonner Springs Shale out of the Wyandotte Limestone and regrouping them as part of the Lane Shale. This reflects the correlation of type Lane Shale to lie between Argentine and Farley Limestones in southeastern Kansas (southwest Johnson County, Miami and Anderson counties). See the text for further discussion of revisions. (B) Generalized stratigraphic section showing the traditional stratigraphic classification into which the Farley Limestone fits (after Arvidson, 1990).

Argentine Limestone Member

The Argentine Limestone is the uppermost member of the Wyandotte Limestone (Figure 2A) and shows great variation in thickness throughout the area (Crowley, 1969; Arvidson, 1990; this study). Crowley (1969) attributed these thickness variations to the presence of a series of phylloid algal banks that attained thicknesses as great as 50 feet (Figure 3). In developing the sequence-stratigraphic framework of the Farley Limestone in this study, the paleotopography on the top of the Argentine Limestone is important because it could have influenced deposition of the Lane-Island Creek shales and Farley Limestone. Arvidson (1990) demonstrated the topographic influence of the Argentine and stated that the Lane Shale is confined to areas where the underlying Argentine Limestone member is thin. Crowley (1969) also demonstrated this topographic influence and stated that the Island Creek Shale extends southward from northern Wyandotte County between areas of thickened Argentine. For these reasons, the top of the Argentine Limestone is included in the correlations and cross-sections developed for this study discussed later.

Lane-Island Creek Shales

Work by Arvidson (1990) indicated that the shales located below the Farley Limestone represent two distinct units and source directions. The isopach maps of Crowley (1969) and this study show that the Island Creek Shale had a northern source and extended southward in a thickened lobe into Johnson County (Figure 4). Arvidson (1990) confirmed this source direction but showed that Crowley misscorrelated the Lane Shale, placing it below the Argentine instead of above. The new correlations of Arvidson (1990), however, also showed that the stratigraphic position of the type Lane Shale between Argentine and Farley Limestones demonstrates its equivalency with the

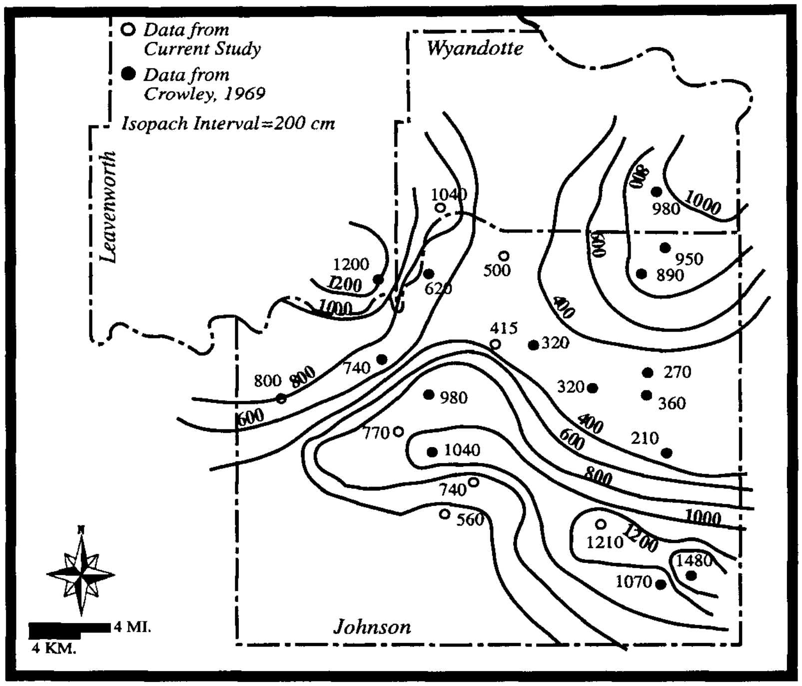

Figure 3. Isopach map showing thickness of the Argentine Limestone within the field area. Data taken from current study and from Crowley, 1969.

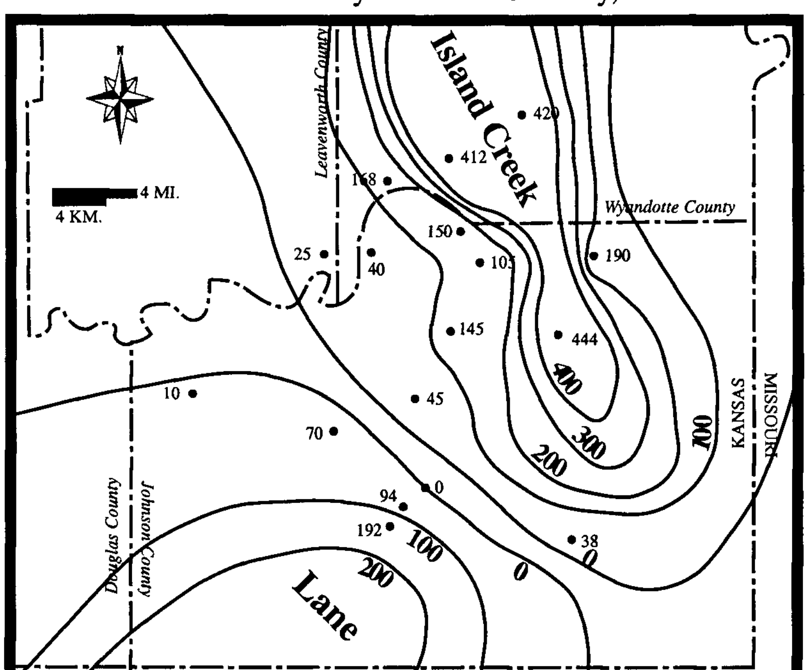

Figure 4. Isopach map showing the thickness of the Lane-Island Creek Shale. Note how thickness of these shale compliments thickness of Argentine Limestone illustrated above. Where the Lane-Island Creek shales are thin the Argentine is thick, and where the Lane-Island Creek is thick the Argentine is thin. Data taken from current study and Crowley, 1969. Isopach interval=100 cm.

Island Creek Shale. Furthermore, Arvidson (1990) argued that the siliciclastic interval separating the Argentine from the Farley in southern Johnson County represents material supplied primarily from southern sources, whereas siliciclastics with a northern source were not deposited here. The work done in the current study confirms that the Island Creek Shale member of the Lane Shale (Figure 2A) does in fact represent two distinct shale units with little to no shale in the areas between them. This distinction of time-equivalent siliciclastics with different source directions is important to make. These siliciclastics are therefore referred to as Lane-Island Creek shales in order to establish that they are time-equivalent but in fact need to be thought of as separate units within the sequence-stratigraphic framework; this distinction is not made in the stratigraphic nomenclature presented in Figure 2A.

Farley Limestone Member

In the area of this study, the Farley Limestone is a mixed siliciclastic-carbonate unit typically composed of three individual submembers (Figure 2A) of varying thickness and lithology; the lower, middle and upper Farley. The lower Farley is a carbonate unit and shows the greatest degree of lithologic and thickness variability. The middle Farley is dominantly siltstone but contains local accumulations of carbonate within it. In the southwest portion of the field area, the middle Farley is composed of a thick accumulation of skeletal carbonate with little to no shale. The upper Farley is exclusively carbonate and is the most lithologically consistent submember. Thickness variability in these units will be discussed in the later parts of this paper.

Bonner Springs Shale

The unit immediately overlying the Farley Limestone at all localities is the Bonner Springs Shale. The uppermost member of the Lane Shale, the Bonner Springs

Shale, contains variable lithologies and thickness (90 cm to 9 m). Lithologies typically observed include mudstone, siltstone, and sandstone (Enos *et al.*, 1989; Crowley, 1969; Arvidson, 1990; this study). Erosional scouring and backfilling as well as the development of a paleosol in the upper few feet of the Bonner Springs Shale indicates widespread subaerial conditions near the end of Bonner Springs deposition (Enos *et al.*, 1989).

Lithofacies & Depositional Environments of the Farley Limestone

The Farley Limestone is divisible into ten distinct lithofacies. All facies were established based on details observed at outcrops, in cores, and in thin sections.

Phylloid Algal Facies

The most common facies in the Farley Limestone is the phylloid-algal facies (Figure 5) that occurs as both boundstone and packstone. Present in all measured sections and cores, this facies is light to medium gray (N5-N7) on fresh exposures and weathered exposures are light brown to grayish-orange (5YR 5/6-10YR 7/4). Where the facies contains large percentages of disseminated argillaceous material (Figure 5d) the rocks have a bluish hue (5B 7/1, 5B 5/1).

Bedding is thin to thick (25 to 100 cm) in scale and is accentuated by thin shale partings. These shale partings commonly contain abundant crinoidal and bryozoan material and are commonly diffused into overlying limestone beds and can account for as much as 30 percent of the rock mass. The main skeletal constituents are phylloid-algal blades, which account for more than 50 percent of the fossils and are present to the exclusion of other fossils in some areas. The phylloid algae have a variety of sizes but typically are wavy veinlets of calcite spar at least 3 cm in length and with lengths up to 12 cm.

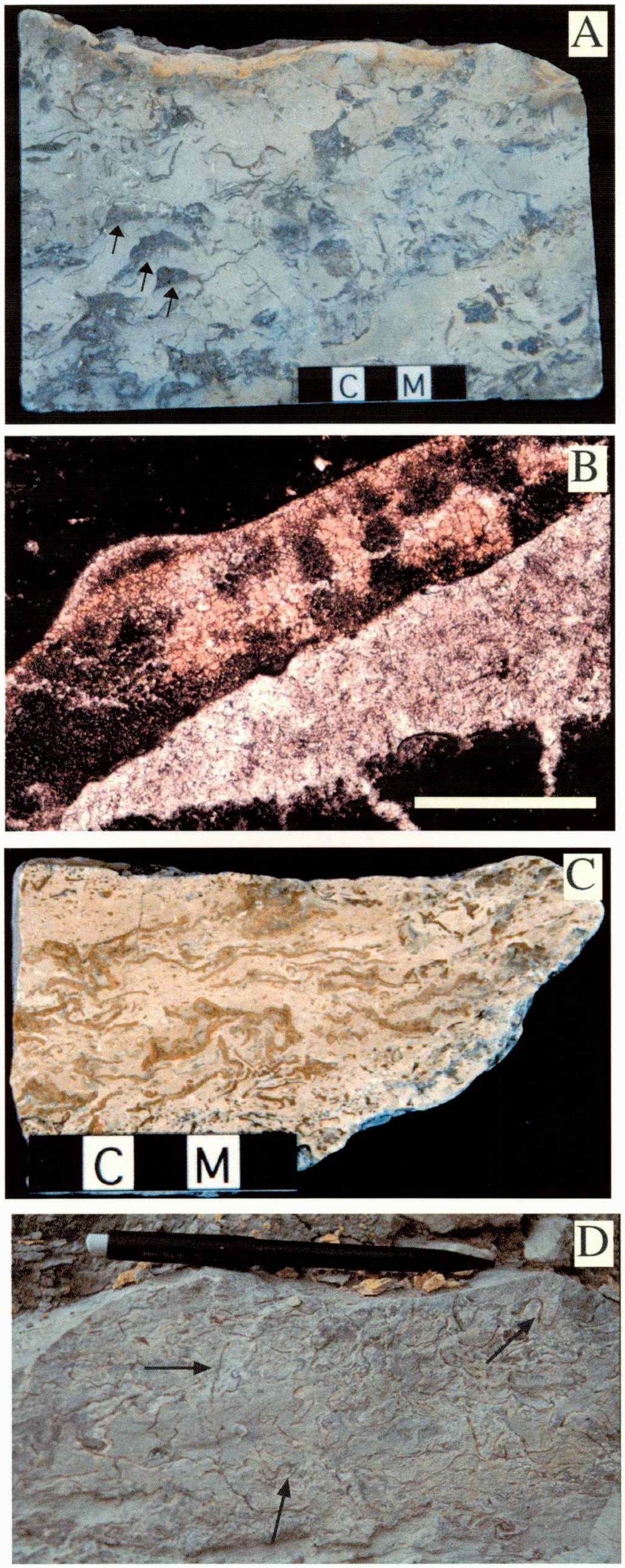

Figure 5 (A) Polished slab illustrating the appearance of the phylloid algal facies. Note the coarse calcite spar filling shelter pores beneath phylloid algal blades (arrows) (sample WR-1).
(B) Photomicrograph of phylloid algal blade with dense micrite above and spar filled shelter pore below (transmitted light; scale =1mm; sample S-7).
(C) Hand sample showing denser packing of lamelar phylloid algal blades (sample RQ-11).
(D) Nature of phylloid algal facies as seen on outcrop. Small wavy veins are phylloid algal blades. (arrows) Bluish color in this particular outcrop is the result of a high percentage of finely disseminated argillaceous material (locality LQ).

The most commonly identified genus of phylloid algae in the Farley Limestone is *Archeolithophyllum* (Figure 6). Other phylloid algae such as *Eugonophyllum* and *Anchicodium* have been identified in the Farley in the past (Crowley, 1969; Harbaugh, 1960; Heckel & Cocke, 1969; Johnson, 1946, 1963; Konishi & Wray, 1961; Wray, 1968) and may be present but unrecognizable due to obliteration of the original structure. The associated fauna is dominated by brachiopods, bryozoans, and crinoids, whereas bivalves, gastropods, small rugose corals, ostracodes, and trilobites are present but much less common.

Shelter pores beneath algal blades (Figure 5 a, b) and phylloid algal molds contain coarse, blocky calcite spar. Fractures are typically filled with blocky calcite spar or in some cases coarse baroque dolomite. The facies generally shows little or no extant, large-scale porosity. In a few locations, however, phylloid-algal blades and other fossils have been leached leaving molds that are lined with light to moderate brown (5YR 5/6-5YR 4/4) residue.

On outcrop and in hand sample, the matrix appears to be homogeneous micrite. Petrographic examination, however, reveals a variety of micrite fabrics dominated by clotted or peloidal micrite. The clots of micrite are approximately 50 to 75 micrometers in size and occur in two forms. The most abundant form is a peloidal micrite sediment that occurs in interparticle and intraparticle spaces. (Figure 7a). The other dominant form is a growth framework that fills interparticle spaces and binds grains together (Figure 6 b, c). Other types of micrite occur as encrustations and micrite envelopes on many skeletal grains (Figure 6d), especially phylloid-algal fragments. Micrite is also present as matrix that has been altered to microspar and pseudospar. These later three types of micrite are less common than the clotted and peloidal forms.

The dominant types of spar within the phylloid-algal facies are interparticle

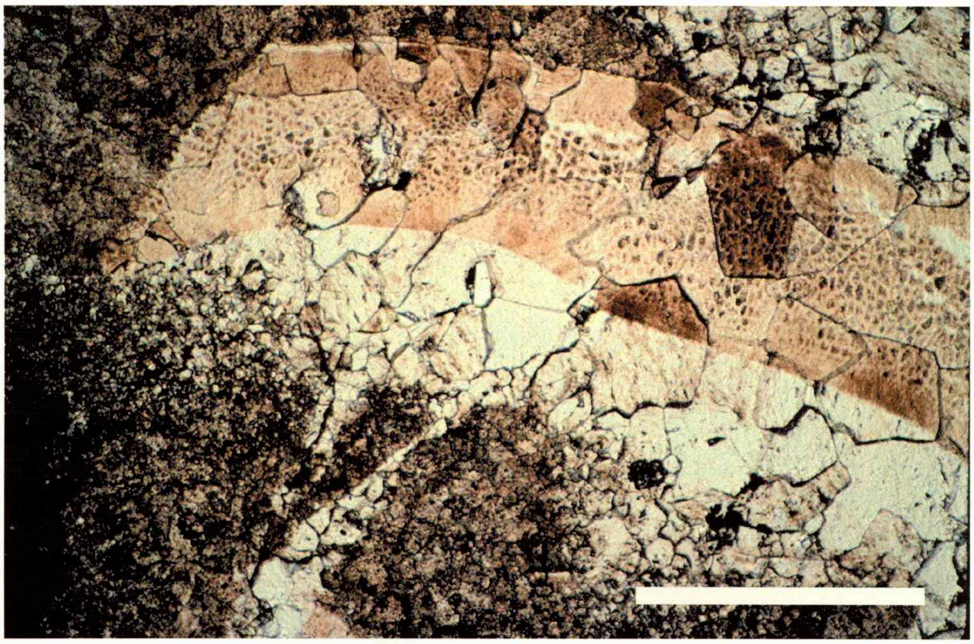

Figure 6 Photomicrograph of *Archeolithophyllum* thalli. Note neomorphic calcite that overprints fabric and preserves the cellular, internal structure (Sample RW-7; transmitted light; scale bar = 1 mm).

cement and neomorphic calcite. Coarse, sparry calcite cement ($\geq$ 0.5 mm) is common in shelter pores and fractures whereas neomorphic spar replaces fossil grains (Figure 6) and is present as an aggrading neomorphic replacement of micrite. Early, fibrous to bladed cements typically line the inside of such fossils as brachiopods and gastropods and are generally overprinted with blocky neomorphic spar (Figure 8). Associated with these early cements is a later partial infilling of micrite or peloidal micrite sediment with a final blocky calcite spar filling the rest of the pore space.

Environmental Interpretation

Wray (1964) interpreted the growth habit of *Archeolithophyllum* as encrusting, locally attached, or free forms that formed semirigid crusts capable of providing a self-supporting skeletal framework and a sediment-binding function in the depositional environment. Furthermore, Wray (1964) compared *Archeolithophyllum* to the modern genus *Lithophyllum*, which is exclusively marine and extensively developed in shallow regions down to approximately 30 meters. By this comparison and, because algae depend on sunlight for important metabolic processes, it is reasonable to infer that the phylloid-algal facies was most extensively developed in shallow water, well within the photic zone. Additionally, other phylloid algae such as *Eugonophyllum* and *Anchicodium* also have been interpreted to live most abundantly in shallow water and effectively baffle and trap carbonate mud as well as to make direct contributions to sediment accumulation in the form of blades, crusts and fragments (Heckel & Cocke, 1969).

The phylloid algae were not likely to have been the only organism trapping and binding sediment. Tsien (1985) discussed possible microbial or bacterial origins of

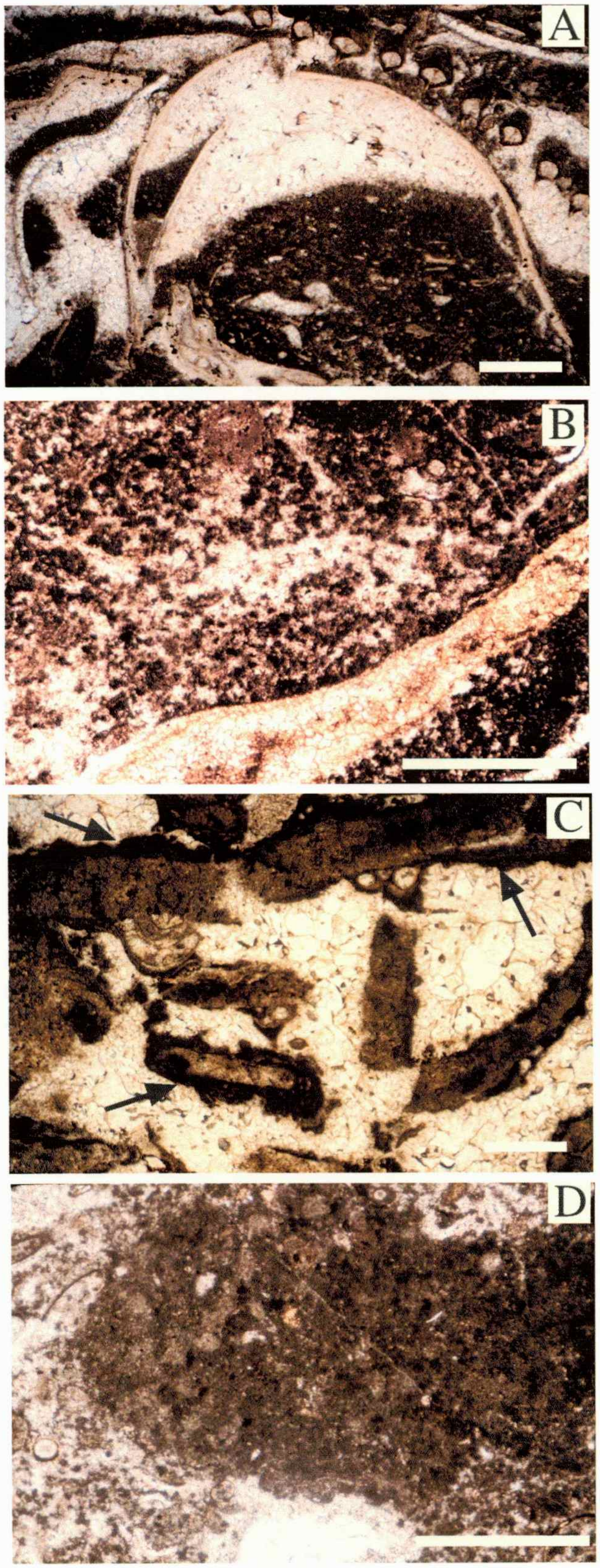

Figure 7 Photomicrographs of dominant micrite fabrics in phylloid algal facies.
(A) Peloidal micrite sediment fills inter- and intraparticle pore spaces and forms geopetal fabrics (Sample BS-7: transmitted light; scale bar = 1 mm).
(B) Peloidal micrite sediment filling interparticle pore spaces (Sample S-7; transmitted light; scale bar = 1 mm).
(C)Micrite encrustation on phylloid algal fragments (arrows) (Sample BS-6; transmitted light; scale bar = 1 mm).
(D) Clotted micrite growth fabrics protrude from grains and in many cases fill interparticle pore spaces, and bind grains together (Sample S-7; transmitted light; Scale bar = 1 mm).

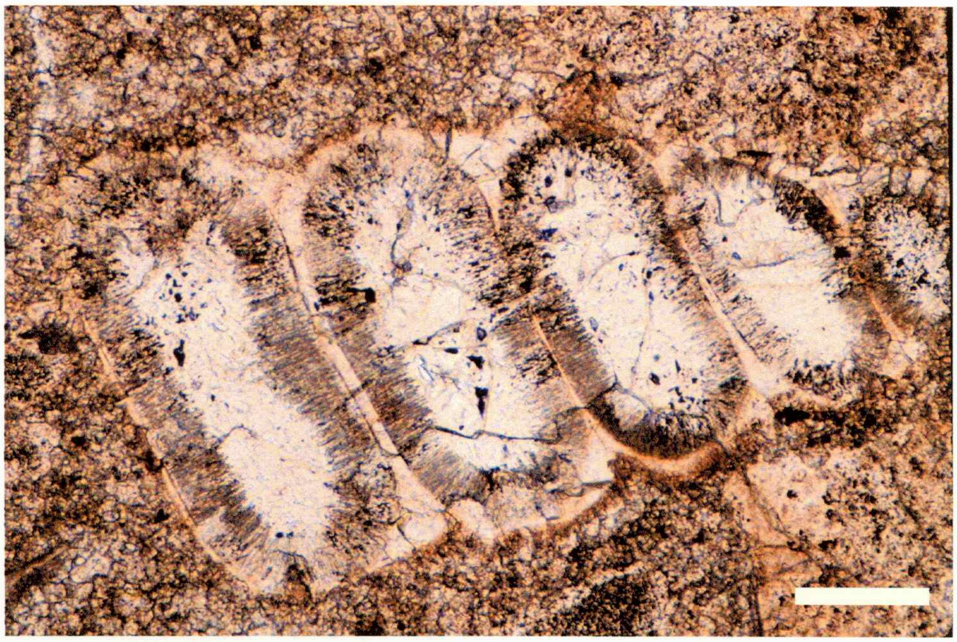

Figure 8 Photomicrograph of gastropod mold lined with early fibrous cement that is overprinted by neomorphic calcite. Original micritic matrix is recrystalized to microspar and some pseudospar. (Sample RW-9; transmitted light; scale bar = 400 micrometers)

micrites stating that patchy, clotted, or irregularly shaped masses may have been associated with decaying organic bodies, forming cryptalgal matlike structures that trapped, stabilized, and supported lime mud. The patchy micritic growth framework with a clotted appearance in the phylloid algal facies forms micrite masses that connect skeletal and phylloid fragments and fill interparticle pore spaces. Therefore, it is reasonable to assume that much of the micrite framework found in the phylloid algal facies is the result of microbial action that facilitated the precipitation and binding of carbonate mud and other carbonate grains.

The inferred growth habits outlined above are often cited in interpretations of depositional environments. The binding and encrusting nature of the algae is cited as evidence that the algae were responsible for the construction of algal mounds or banks. These banks resulted from the growth and proliferation of phylloid algae on and around topographic prominences. Harbaugh (1964) stated that, initially, algal mounds may have been localized by waves and currents that caused both argillaceous and calcareous material to be heaped into submerged bars. These bars then became nucleation sites for growth of phylloid algae. Heckel and Cocke (1969) supported this idea, saying that local sedimentary highs on an irregular sea floor provided favorable locations for growth of phylloid algae because sunlight was favorable for algal growth. Once established, the growth and proliferation of the algal community built up local phylloid algal mounds or banks.

Ball *et al.* (1977) offered an alternate interpretation and argued strongly against the concept of phylloid algae as mound or bank builders. They stated that phylloid algae were not builders of depositional topography but rather were only a source of building material. They went on to say that there is no evidence for the ideas that phylloid algae were commonly significant sediment bafflers or that they were ever important bank or mound builders in Pennsylvanian and Early Permian seas. In fact, the proliferation of phylloid algae or at least the environment where the greatest quantities of their transported remains occur, apparently was in broad, shallow embayments between contemporaneous deltaic depocenters (Ball *et al.*, 1977).

Although those on both sides of the argument are able to present evidence to support their conclusions, a combination of the two interpretations best serves to explain the distribution of phylloid-algal facies found in the Farley Limestone. Evidence for both models will be presented later in this paper.

Skeletal Wackestone-Packstone

The skeletal wackestone-packstone facies (Figure 9) consists of thin to medium-bedded (25 to 50 cm) medium- to light-gray (N5-N7) deposits. This facies is differentiated from the phylloid algal facies by a much lower percentage of phylloid-algal remains, typically around 15 to 20 percent of the total fauna, and a higher density of associated fauna. The skeletal wackestone-packstones also exhibit thinner average bedding (35 cm) than the phylloid algal facies. The most common skeletal constituents include both whole and fragmental brachiopods, bryozoans, crinoids, fusulinids, and gastropods as well as other unidentified skeletal fragments. Phylloid algae are present but typically occur as fragments of 5 cm or less and show no cellular preservation. Instead, the phylloid algal fragments occur as molds of algal thalli that have been filled with blocky calcite spar.

The dominant depositional fabric observed in hand samples is packstone. Patches of densely packed skeletal remains are often observed within individual thin sections (Figure 10). The accumulations range in size from 2-3 mm to 3-5 cm in both length and width.

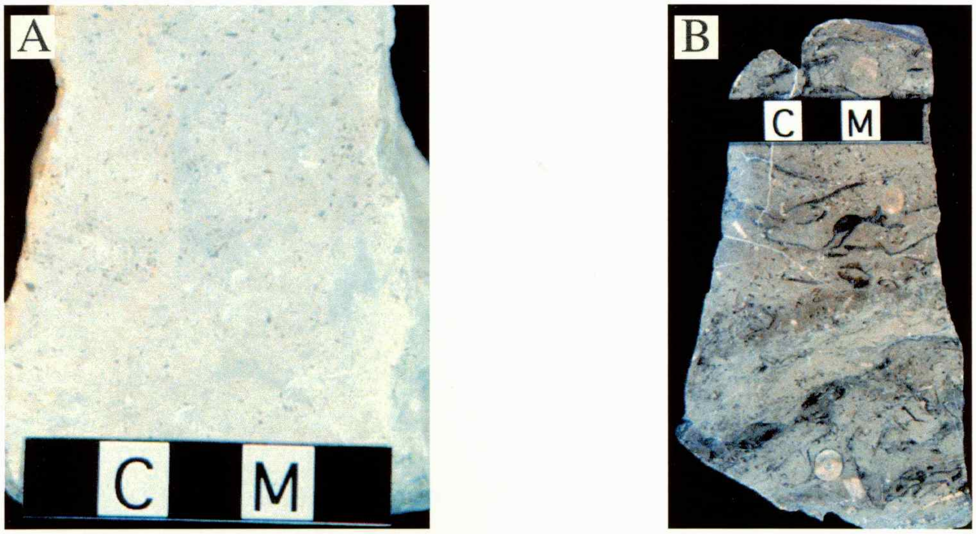

Figure 9. Hand samples showing skeletal wackestone-packstone facies. (A) This sample contains dominantly fine-grained skeletal material and so appears to be a mudstone in hand sample. See Figure 2.10b for photomicrograph showing true fabric (sample BS-4); (B) This sample demonstrates the more typical expression of the facies with coarser skeletal material and fragmental phylloid algal remains (sample RW-2).

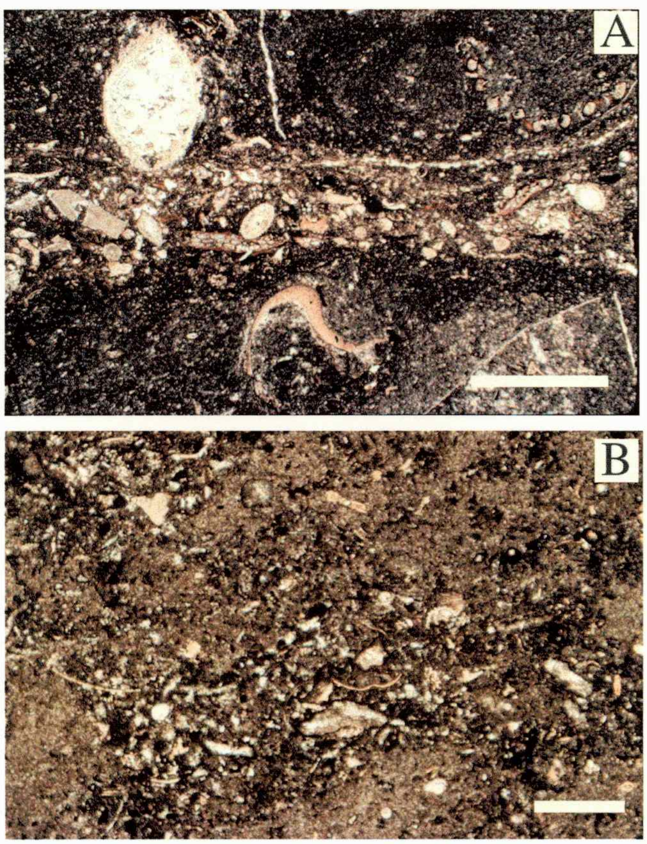

Figure 10. Photomicrographs showing various skeletal wackestone-packstone fabrics. (A) This sample exhibits depositional micrite matrix with densely accumulated skeletal material in a linear arrangement. This likely represents a burrow filled with skeletal material (sample RW-5; transmitted light; scale bar = 2 mm). (B) Skeletal wackestone with depositional micrite matrix and fine grained skeletal material Photomicrograph taken from hand sample shown in Figure 2.9a (transmitted light; sample BS-4; scale bar = 1 mm).

Although present in a few thin sections, the clotted micrite fabric, which dominates the phylloid-algal facies, is much less common in the skeletal wackestone-packstone facies. Instead, the matrix is dominantly depositional micrite that has been recrystallized to microspar (Figure 10). Coarse spar is found filling fractures and geopetal cavities, but overall the facies contains a much smaller percentage of coarse spar than does the phylloid algal facies (15 to 25 percent in the skeletal wackestone-packstone facies versus 25 to 50 percent in the phylloid algal facies). The skeletal wackestone-packstone facies is similar to the phylloid-algal facies in terms of its distribution of amount of argillaceous debris.

Environmental Interpretation

The matrix of the skeletal wackestone-packstone facies is dominantly depositional micrite. The facies lacks abundant phylloid algae or abundant microbial micritic framework that would have trapped and bound carbonate mud. Therefore, the skeletal wackestone must have been deposited in a low-energy environment that allowed the deposition of fine carbonate matrix.

The diverse, unabraded fauna provides further evidence of a quiet, open-marine environment. The presence of organisms such as bryozoans, brachiopods, echinoderms, and corals indicates a marine environment of normal salinity (Heckel, 1972b). Additionally, the irregular patches of skeletal packstone in the facies are evidence of bioturbation with patches of dense skeletal material that probably represent the accumulation of skeletal material in burrows. It has been shown that these irregular patches of packstone-grainstone in modern settings may be produced by storm infilling of excavated burrow systems (Tedesco & Wanless, 1989).

Peloidal, Skeletal Packstone Facies

The peloidal, skeletal packstone facies (Figure 11) exhibits a wide range of thicknesses (10 to 210 cm). On outcrop the bedding is thin to medium in scale ranging from 20 to 80 cm. The peloidal, skeletal packstone typically is yellowish to light gray (5Y 8/1-N8) both on fresh outcrops and in cores. The peloidal, skeletal packstone facies typically contains less than 3 percent silt and clay. The main constituents are peloids and skeletal fragments of brachiopods, bivalves, gastropods, bryozoans, crinoids, phylloid algae, and corals. Micrite matrix is present in all occurrences but most are matrix poor (approximately 3 to 5 percent matrix). Grain sizes are variable (100 microns to centimeters) but within each occurrence the constituents tend to be well sorted and show no preserved, physical sedimentary structures. Nearly all grains show some level of micritization from a thin envelope to complete replacement (Figure 12).

This facies contains a small percentage of extant interparticle and intraparticle porosity (3 to 5 percent) but most original porosity has been filled with blocky calcite spar or micrite. Early cements are bladed to fibrous spar found mainly in brachiopods and gastropods. The majority of the spar in this facies is equant blocky calcite cement that fills nearly all interparticle and intraparticle porosity. Because nearly all interparticle and intraparticle porosity has been filled with cement, the total percentage of the rock composed of spar is approximately 60 to 75 percent. The average crystal size, however, is small at approximately 0.5 mm.

<u>Environmental Interpretation</u>

The relatively small amount of micrite matrix suggests that energy levels were too high to allow deposition of fine carbonate sediment. Therefore, this facies represents a higher-energy environment than that found in the skeletal wackestone-

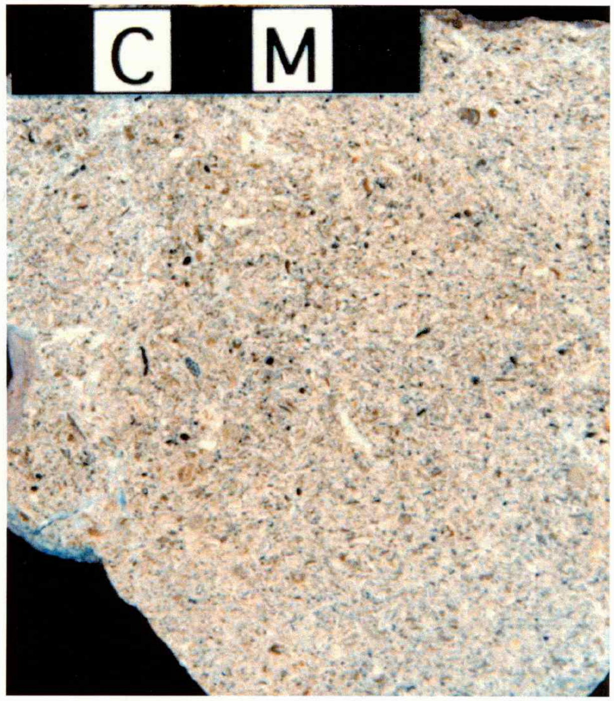

Figure 11. Hand sample showing fabric of peloidal, skeletal packstone facies (sample BS-19).

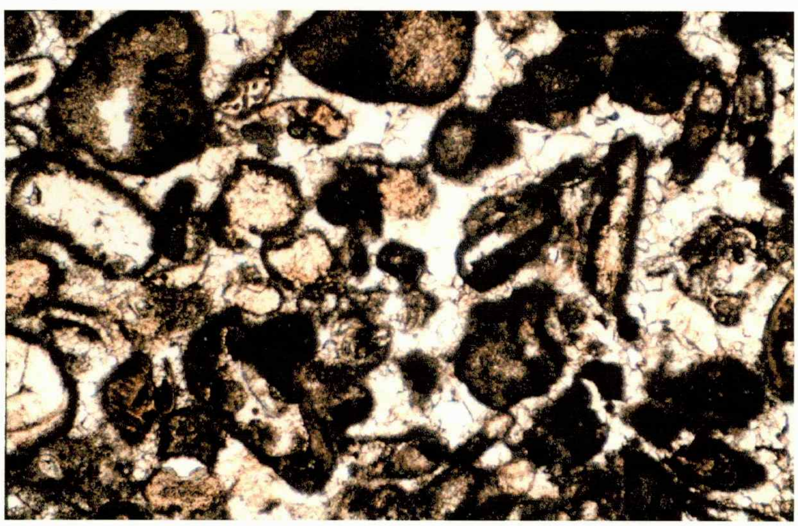

Figure 12. Photomicrograph of peloidal, skeletal packstone facies. Note the micritization in various stages of development from thin envelopes to complete replacement. Interparticle porosity is filled with equant, blocky cement (sample BS-19; transmitted light; scale bar = 500 micrometers).

packstone facies or phylloid-algal facies. The presence of abundant, well-developed micrite envelopes on nearly all grains also suggests a shallow-water, protected environment where intensive boring by microorganisms was common (Golubic *et al.*, 1975). The lack of physical sedimentary structures in the peloidal, skeletal packstone facies indicates energy high enough to transport and wash sediment but perhaps not continuous enough to prevent sedimentary structures present from being destroyed by bioturbation.

Sandy, Sketetal Grainstone-Packstone Facies

Found at only a few localities in the study area, the sandy, skeletal grainstone-packstone facies (Figure 13) has several distinctive features. Bedding varies from horizontal beds to medium-scale cross bedding (Figure 14). The cross beds (Figure 14a) are typically 15 to 30 cm thick and have variable apparent dips from 8 to 35°. Where the beds are horizontal, the are approximately 30 to 50 cm thick. The sandy, skeletal grainstone-packstone facies typically occurs as medium to medium-dark gray (N5-N4), silty to sandy beds that contain abundant, coarse fossil debris. The cross-beds are concave upward and in places truncate the beds below them. Where bedding is horizontal, there is a higher abundance of micrite and fine sand and silt.

The main skeletal constituents include brachiopod, bivalve, gastropod, algae, bryozoan, and crinoid fragments. Some nonfragmental fossils and whole fossil molds are present and typically are gastropods. In hand samples and in thin sections most elongate skeletal particles, such as brachiopod and bryozoan fragments tend to be oriented parallel (Figure 13). Also visible in some hand samples is grading with concentrations of coarser particles near the base of beds (Figure 13). In addition to the skeletal fragments, silt- and sand-sized quartz grains, peloids, and plant fragments

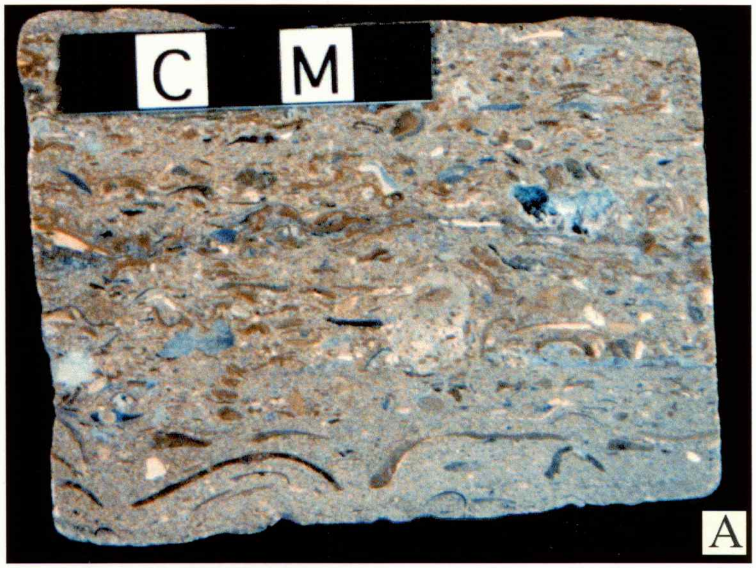

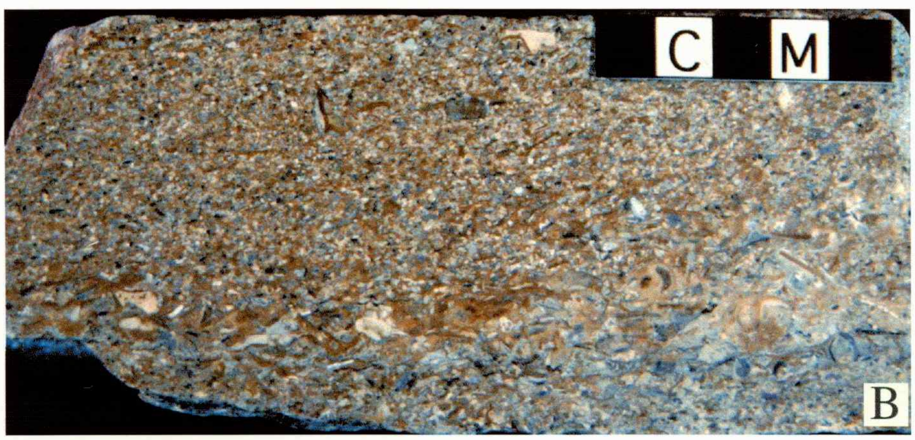

Figure 13. Hand samples showing nature and details of sandy, skeletal grainstone-packstone facies. (A) Hand sample showing general parallel orientation of elongate skeletal grains (sample S-10). (B) Hand sample that exhibits slight grading with coarsest grains concentrated at the base and finer particles distributed throughout the upper part of a bed (sample HM-7).

Figure 14. Outcrop photos of sandy, skeletal grainstone-packstone facies. (A) Cross-bedded sandy, skeletal grainstone-packstone as observed at locality HM (See figure 2.1 for locality map). Staff is 1.5 m. (B) Horizontal bedding in sandy, skeletal grainstone-packstone facies as observed at locality SRO (see figure 2.1 for locality map). Some trough cross bedding is present (arrow) but is truncated by overlying horizontal beds.

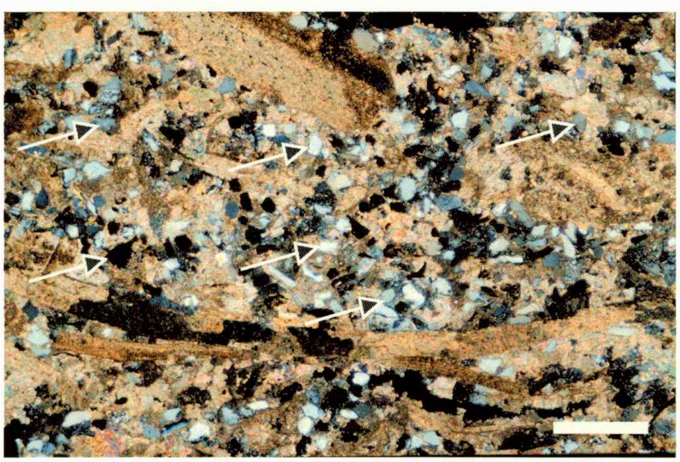

Figure 15. Photomicrograph of typical fabric of sandy, skeletal grainstone-packstone facies. Note abundance of coarse skeletal fragments. Also note the abundant fine sand-silt sized quartz grains (arrows) (sample S-7; plane polarized light; scale bar = 1 mm).

of various types and sizes are common. Plant fragments are typically oriented parallel to bedding planes in thin layers. Micritized grains are present but much less common than in the peloidal, skeletal packstone facies (Figure 15). The above described features allow the sandy, skeletal grainstone-packstone facies to be differentiated from the peloidal, skeletal packstone facies.

Environmental Interpretation

The association of terrigenous material such as detrital quartz and plant material with marine skeletal debris in the sandy, skeletal grainstone-packstone suggests the close proximity of a terrigenous source to a marine environment. Because of this relationship, it seems most reasonable to interpret the sandy, skeletal grainstones and packstones found in the Farley as either distributary channel or distributary mouth bar deposits.

Deposition within tidal channels is one scenario. Medium-scale cross-beds like those found in the sandy, skeletal grainstone-packstone facies are characteristic of tidal channels in nearshore environments (Wilson & Jordan, 1983). Another possibility is deposition as a distributary mouthbar. Reineck and Singh (1975) stated that distributary mouth bars are sandy shoals formed near the seaward limit of distributary channels. Deposits of distributary mouth bars are made up of sand and silt, commonly with thin laminations of plant debris. The most common sedimentary structure is trough cross-bedding (Reineck & Singh, 1975).

Oolite Facies

Oolite (Figure 16) occurs in several localities throughout the Farley Limestone. There are two types of oolite in the Farley Limestone, and they each comprise an oolite subfacies. The first type is ooid grainstone. The greatest accumulation of this subfacies is towards the north where the lower Farley is composed of a single bed of cross-bedded oolite (Figure 17 & 18b). This weathered outcrop is light to yellowish gray (N7-5Y 7/2). Other oolites to the south and southwest are composed of single, thin (15 to 55 cm) beds that show no cross-bedding. Cross-bed measurements taken in the north, indicate two dominant paleocurrent directions, one to the southeast and the other to the northwest (Figure 18). Ooid grainstones are also present as thin accumulations that are not cross-bedded.

Ooid sizes in ooid grainstone subfacies range from 0.5-1.5 mm. The deposits are well sorted and overpacked with slight grain suturing in places. Ooid cortices are dominantly fine quartz grains and skeletal fragments. Coarse-grained fossil material is rare to absent within the oolite grainstones. Fossil fragments, commonly encrusted by algae, are common. Cements are composed of equant, blocky calcite, and there is slight micritization of ooids and other grains. Oomoldic porosity is well developed in the northernmost ooid grainstones where ooid cortices have been leached away.

The oolitic, peloidal packstone subfacies are massively bedded accumulations that show no preserved sedimentary structures. Ooid and peloid sizes range from 150 to 1,000 microns and sorting is generally poor to moderate. Ooid cortices are unidentifiable due to replacement by blocky, equant calcite spar. Micrite envelopes on ooids are common and commonly completely micritize the grains (Figure 19).

Keystone vugs are common in the oolite, peloid packstone facies. These fenestrate and other interparticle pore spaces are lined with micrite cement that shows meniscus fabrics and fabrics similar to pendant cement. There is also a later isopachous fringe of bladed calcite cement around the grains and lining vugs. The final pore fill is coarse calcite spar or in some cases coarse baroque dolomite (Figure 19).

All occurrences of oolite are virtually free of shale or fine siliciclastic material. There are no shale partings between bedding planes and no diffuse argillaceous material.

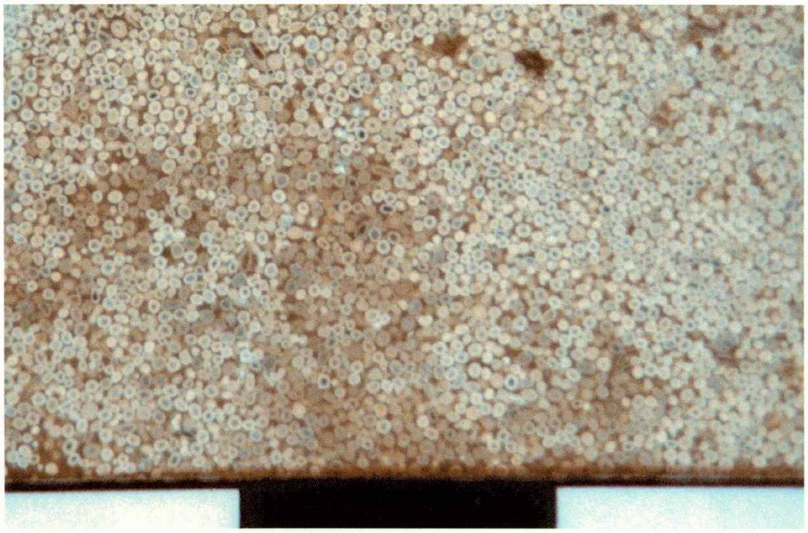

Figure 16. Detail of ooid grainstone from locality C6. Ooids in this locality (see Figure 2.1 for locality map) are well sorted and smaller relative to ooids found to the north. Scale bars are 1 cm each.

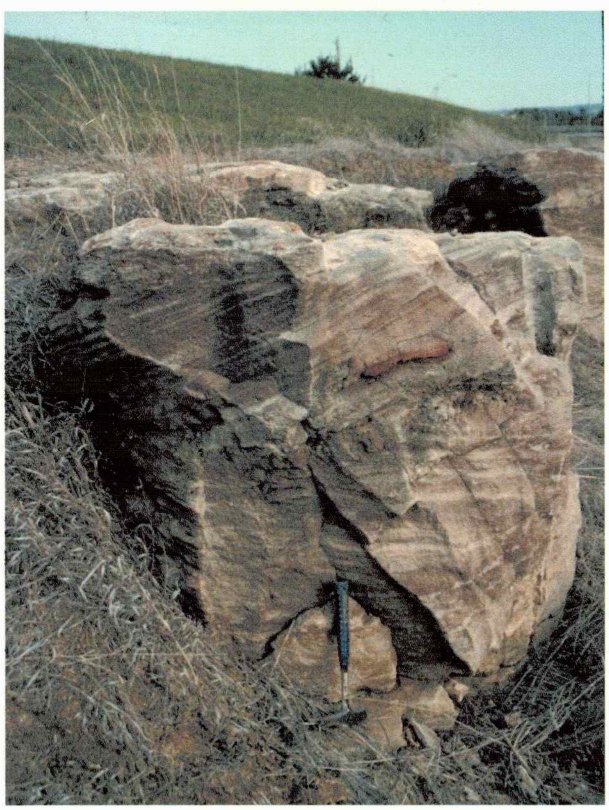

Figure 17. Outcrop of cross-bedded ooid grainstone in lower Farley at locality MCI (see Figure 2.1 for locality map).

(A)

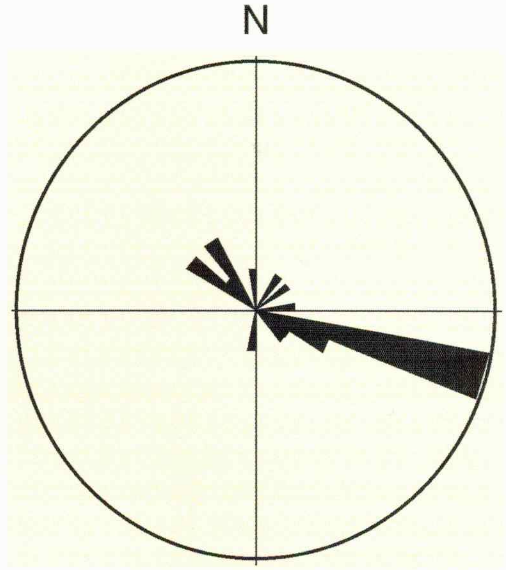

Figure 17. (A) Rose diagram illustrating paleocurrent directions as measured from cross-bed orientation data. Based on 20 measurements collected from the lower Farley oolite at locality MCI. (B) Outcrop photo of cross-bedded oolite at locality MCI (see figure 2.1 for locality map). Note the variable cross-bed directions.

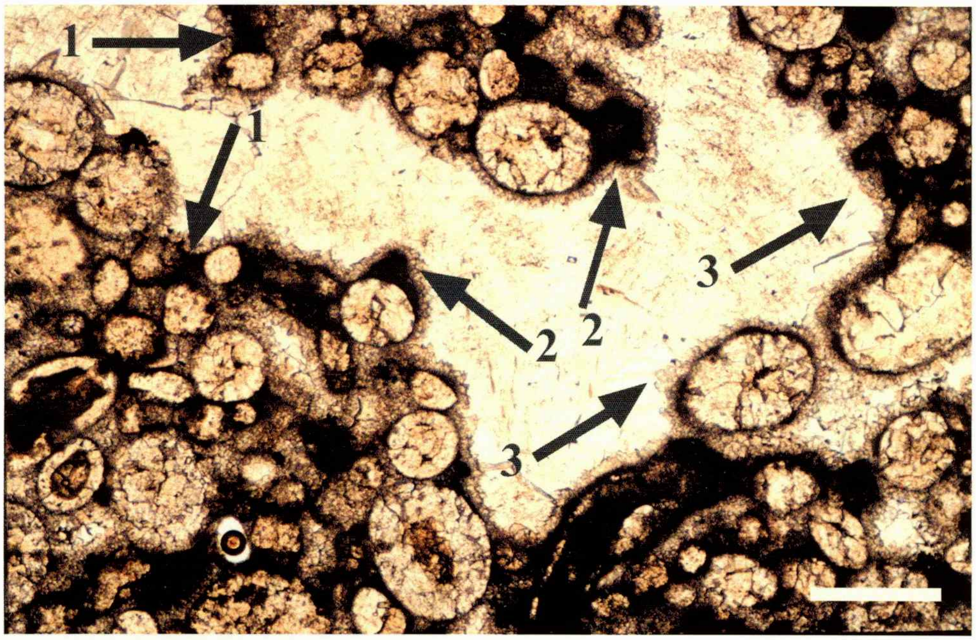

Figure 19. Photomicrograph of ooid, peloid packstone with large keystone vug. Note the micritic cement showing meniscus (1) and an asymmetric fabric similar to pendant cement (2). Also note the later isopachous fringe of bladed calcite cement (3). Final pore fill is coarse baroque dolomite and calcite spar (transmitted light; sample BS-3; scale bar = 500 micrometers).

Environmental Interpretation

Harris (1984) described modern accumulations of several oolite facies around Joulters Cay on the Great Bahama Bank, including oolite grainstone and fine-peloid packstone that contains peloids, micritized ooids, and skeletal fragments. These two modern facies are similar to the oolite subfacies described from the Farley Limestone. Harris (1984) reported that fine-peloid packstones containing ooids accumulated in protected lows and that ooid grainstones formed on bedrock highs where bottom agitation was focused.

Although slight differences exist, an analogy between these modern oolites and oolites in the Farley Limestone is supportable. The micrite-free oolite grainstones are cross-bedded and represent deposition in the highest energy waters. Alternatively, the ooid, peloid packstones represent deposition in protected areas or deeper-water areas that had lower energy levels. Diagnostic indications of shallow water for the ooid, peloid packstone subfacies include the presence of keystone vugs and meniscus fabrics as well as, asymmetric pendant-like fabrics. These fabrics indicate cementation in the presence of water and air such as occurs in the marine or phreatic vadose zones (Tucker, 1991).

Osagia-*Brachiopod Packstone Facies*

Located within a single bed (30 to 95 cm thick) at the base of the upper Farley, the *Osagia*-brachiopod packstone facies (Figure 20) is a marker bed and is useful for correlation. It is medium to medium-light gray (N5-N6) at the base and commonly has a color change to lighter gray toward the top (N7). This facies is distinguished by a zone of skeletal material and whole brachiopods, typically *Composita*.. Other than the *Composita* there is little to no other coarse skeletal material. The brachiopods are typically encrusted by *Osagia* (Figure 20, 21). Johnson (1963) described *Osagia* as colonies that consist of twisted tubes of varying sizes that form a laminated encrustation around a nucleus of fossil fragment or other foreign substance. The smaller tubes have dark walls and, in some examples, cross partitions. *Osagia* has been found to consist of an intergrowth of small tubular algae, similar to *Girvanella*, and the encrusting foraminifer *Nubecularia* (Johnson, 1963).

In the Farley, these encrusting masses completely or partially encrust grains of all types but seem to be most commonly found on whole brachiopods, brachiopod fragments, and phylloid-algal fragments. The coatings have a wide range of morphologies. In some samples they are irregular, thick, asymmetrical coatings, whereas in other occurrences they are symmetrical, thinly laminated coatings. The *Osagia* coated grains can be found throughout the bed but typically occur in the middle to upper half of the bed.

Environmental Interpretation

The wide distribution and consistent stratigraphic location and facies character of the *Osagia*-brachiopod packstone facies suggests that at the time of its deposition the environment was similar throughout the study area. Ginsburg (1960) reported that modern oncolites are formed in low intertidal and shallow subtidal zones and interpreted a similar environment for *Osagia*. Wilson (1970) indicated that oncolitic coatings commonly form in restricted marine bays and lagoons. Asymmetrical coatings of *Osagia* develop when the nucleus on which the coating is growing is occasionally overturned by wave action allowing growth to continue on a new surface (Ginsburg, 1960).

In the current study, the presence of *Osagia* coatings on all sides of a skeletal grain indicates an energy level just strong enough to overturn occasionally the grains

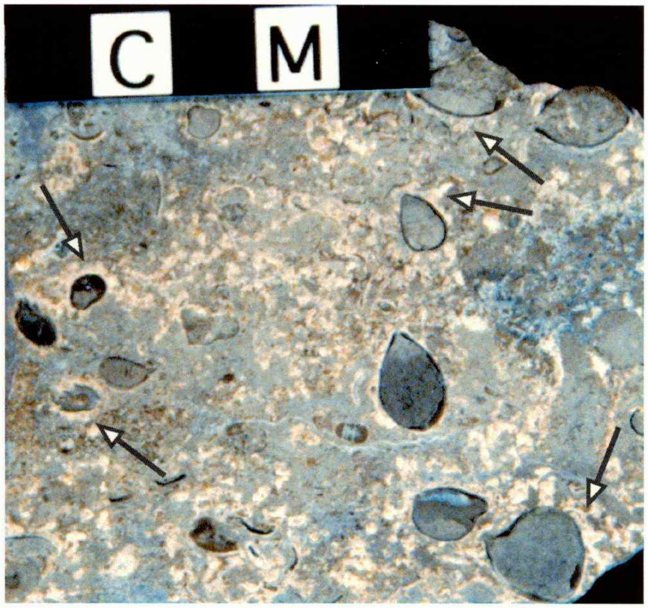

Figure 20. Hand sample of *Osagia,* brachiopod packstone facies. *Osagia* coatings are easily visible as white coatings on skeletal fragments and whole fossils (arrows). Also note the abundance of dense micritic matrix (sample BS-5).

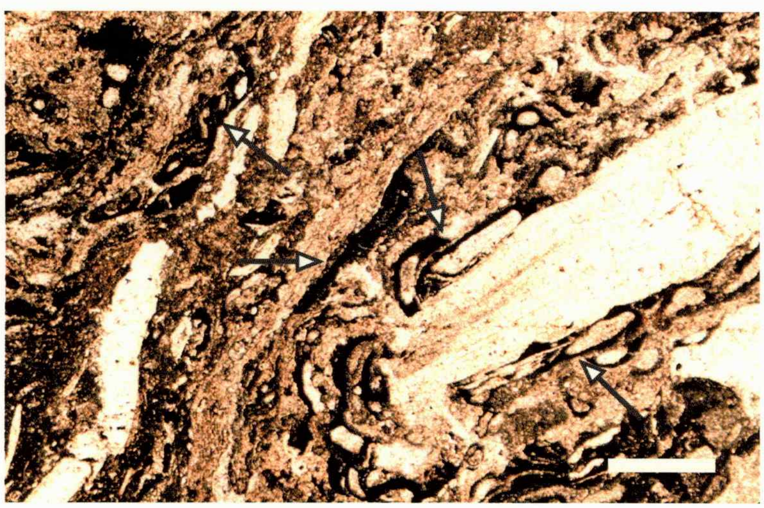

Figure 21. Photomicrograph of *Osagia,* brachiopod packstone facies. Note the large brachiopod fragment with a coating of *Osagia* (arrows) recognized by the chambers (typically spar-filled) surrounded by dense (black) algal growth (transmitted light; sample SH-8; scale bar = 1 mm).

supporting the algal coatings. In many cases the *Osagia*-coated grains are skeletal fragments and small brachiopods that would not have required significant wave energies to move them. Furthermore, the abundance of micrite matrix suggests a moderate to low-energy environment as does the preservation of brachiopods articulated valves. Furthermore the presence of a low-diversity fauna dominated by *Composita* brachiopods indicates a somewhat restricted environment (Ramsbottom, 1978).

Fossiliferous Siltstone

Richly fossiliferous siltstones occur in the Farley and Lane-Island Creek shales throughout the study area. The fossiliferous siltstones represent the thinnest (20 to 150 cm thick) overall accumulations of siltstone in the Lane-Island Creek and middle Farley. They have a platy to blocky texture and a light bluish-gray to medium-gray color (5B 7/1-N5) on outcrops and in cores. The siltstones are highly calcareous and slightly micaceous and have no sedimentary structures, although burrow molds are present in some outcrops (Figure 22).

Most fossil material is fragmental although there are whole brachiopods, gastropods, and bivalves in some localities and the fossiliferous texture shows up best in weathered sections (Figure 23). In cores the fossiliferous siltstones are blocky to massive and contain variable amounts of fossil material (Figure 24). In the Lane-Island Creek, these fossiliferous siltstones are dominated by crinoid ossicles and calyx plates as well as articulated crinoid columnals, with brachiopods and fenestrate and ramose bryozoans also abundant. Fusulinid foraminifera are also present in minor amounts in two sections in the Island Creek. In the middle Farley siltstones, the fossil assemblage is dominated by fenestrate bryozoans and brachiopods with crinoids, bivalves, and gastropods present but less abundant.

Environmental Interpretation

Crinoids and other echinoderms are stenohaline, and their remains are originate in sediments of fully marine origin (Clarkson, 1993). Brachiopods are also normal-marine organisms, whereas bryozoans are able to survive in restricted conditions; but they prefer normal-marine environments (Heckel, 1972b).

We interpret the environment of the fossiliferous siltstones as one of normal marine salinity and low energy levels. The most likely situation that gave rise to the fossiliferous siltstone facies is deposition in areas between the Lane and Island Creek deltas and in areas distal to the middle Farley delta. In these deeper areas between or distal to thickened delta lobes, water was clearer and calmer; and a normal-marine fauna could exist. Occasionally, influxes of large quantities of silty material from the deltas swamped and buried the organisms. Following this, the fauna recovered and bioturbation destroyed sedimentary structures and disrupted and disarticulated the buried fossils.

Lenticular Bedded-Laminated Siltstone and Fine Sandstone

Siltstones with millimeter- to centimeter-scale lamination and lenticular bedding occur in both the middle Farley and Lane-Island Creek shales. The nature of this facies is most visible in cores (Figure 25) and on very fresh outcrops. On weathered outcrops this facies appears as a platy to fissile, fine sandstone to siltstone (Figure 26). Colors vary with grain size with the siltstone being medium-light to medium gray (N6-N5) and the sandstone very light gray to light gray (N8-N7). The siltstone is noncalcareous, but the sandstone lenses and laminations are slightly calcareous. Fine sand-sized and coarser mica grains are abundant in this facies and are most visible in cores and on very fresh outcrops.

Figure 22. Burrow molds taken from fossiliferous siltstone facies. Burrows are distinguished by their circular to ellipsoid cross-section and are typically filled with fine sand and have silt and sand accreted to the outer surfaces (locality WR). Penny for scale.

Figure 23. Outcrop surface of fossiliferous shale. Note abundant fossil material including crinoid ossicles (1), ramose bryozoans (2), and brachiopod (3) fragments (locality WR) . Penny for scale.

Figure 24. Core section showing nature of fossiliferous siltstone facies. Fossil fragments are white (arrows) in core and the siltstone is blocky to massive. Also visible are horizontal burrows (B); (locality C5).

The lenticular bedding observed in cores and on fresh outcrops is the result of millimeter- to centimeter-scale laminations and lenses of fine sandstone within the finer siltstone. Faint, millimeter-scale ripple cross-laminations occur in the sand lenses in core and on fresh outcrop. Although no body fossils are present in this facies, horizontal burrow molds occur in most sections (Figure 25). The burrows are most visible in core and appear as circular to ellipsoid sandstone lenses in cross-section. These burrow forms typically distort and cross-cut laminations and lenticular bedding. The abundance of burrows is greater in the Island Creek siltstones, whereas the middle Farley siltstones have fewer burrows and much finer laminations (2 to 8 mm in the middle Farley v. 5 to 15 mm in the Island Creek) and lenticular bedding (Figure 25).

Environmental Interpretation

Reineck and Singh (1980) stated that lenticular bedding requires conditions of current or wave action depositing sand, alternating with slack-water conditions when mud is deposited. Furthermore, they concluded that it occurs primarily in subtidal zones and intertidal zones. Lenticular bedding is also a common feature of delta-front environments where sediment supply and flow strength fluctuate (Tucker, 1991).

Sedimentary structures similar to those observed in the middle Farley and Lane-Island Creek are found in the modern Mississippi delta. Moore and Scruton (1957) noted the presence of laminated to lenticular bedded sediments (their regular to irregular layers) in the Mississippi delta and they noted that these structures were present in two bands of sediments surrounding the delta in waters 6 to 300 feet deep. Additionally, they noted that such fine sedimentary structures as laminations and lenticular bedding are highly vulnerable to destruction and are most likely to be preserved in an environment which has rapid deposition or very few organisms (Moore and Scrunton, 1957).

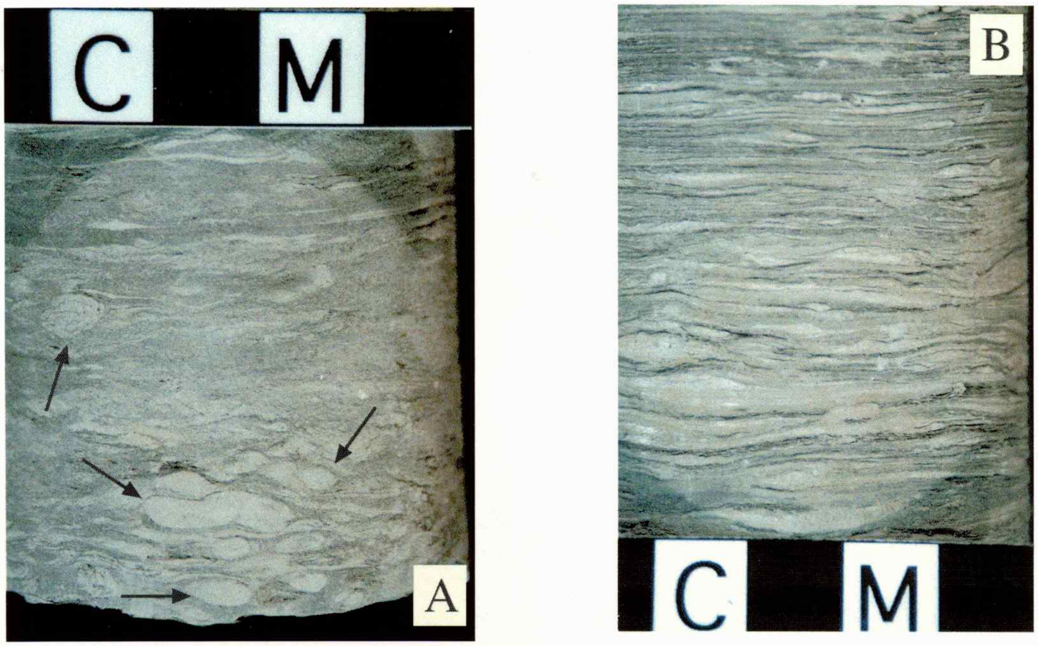

Figure 25. Core sections showing the fabric of the laminated to lenticular bedded siltstone and fine sandstone facies. (A) This core section from the Island Creek Shale contains abundant horizontal burrow molds (arrows) that disrupt laminations and lenticular bedding. (Core #3)
(B) This core section from the middle Farley shows finer laminations and contains fewer burrows. (Core # 3)

Figure 26. Photo showing nature of laminated to lenticular bedded siltstone to fine sandstone facies as it appears on weathered outcrop. Typical expression is as a platy to slightly fissile siltstone to fine sandstone. Ripple cross-laminations are rarely visible except on very fresh outcrops.

Shepard (1964) also discussed the presence of well-laminated sediments in the delta front of the Mississippi and stated that delta facies can be recognized by the abundance of lamination and the scarcity of marine organisms. Whereas the presence of burrows, especially in the Island Creek-Lane, indicates some bioturbation, the abundance of preserved sedimentary structures suggests rapid deposition that outpaced bioturbation. Therefore, it is most likely that the laminated to lenticular bedded siltstones and fine sandstones present in the middle Farley and Lane-Island Creek represent accumulations of marine, tidally dominated delta front to prodelta sediments rapidly deposited in shallow water or perhaps in depths to approximately 80 meters.

Organic-rich Mudstone and Coal

Darkly colored mudstones with high concentrations of plant debris, rootlets and organic matter occur in the southern part of the field area. These thin mudstones (15 to 50 cm thick) range in color from olive gray to grayish black (5Y 4/1-N2). The deposits are blocky to massive and not fissile. Also, there is a thin coal (2 to 5 cm thick) which may grade upward to typical dark mudstone. In addition to the abundant plant debris and rootlets, there is a fauna of very small (1 cm or less) bivalves. These fossils are rare and are the only body fossils observed.

Environmental Interpretation

Dark gray to black shales of the Midcontinent are typically attributed to deposition in deep, anoxic waters far offshore (Heckel, 1977). These deep-water black shales are typically fissile and contain phosphate, pyrite, and an abundance of such pelagic fossils as conodonts and ammonoids (Heckel, 1977). The dark organic-rich mudstones described in the current study, however, are not fissile and do not contain phosphate or pelagic fossils.

It appears more likely that the dark organic-rich mudstones described herein were deposited in a brackish marsh or lagoonal environment. Lagoonal bottom sediments are muddy and black with hardly any traces of primary bedding visible due to bioturbation (Reineck & Singh, 1975). Reducing conditions within lagoonal environments are characterized by abundant well-preserved plant debris (Reineck & Singh, 1975) such as is preserved in the organic-rich mudstone and coal facies of this study. The thin coal seam in this facies further supports the interpretation of a lagoonal environment as does the absence of abundant and diverse fauna. The rare body fossils are small and probably are a restricted, dwarfed fauna.

Blocky Mudstone

Blocky mudstones (Figure 27) are present in the middle Farley and the Island Creek Shale. In all occurrences the blocky mudstones are noncalcareous and comprise fine silt to clay with abundant mica. Colors typically range from medium, light gray (N6) to light olive gray (5Y 6/1) on fresh outcrops and in cores. Weathered outcrops have a large variety of colors with mottling common. Additional colors observed include shades of brown, olive green, and bluish gray.

The mudstones of the middle Farley are massively bedded and exhibit irregular curved fractures on outcrops. Hand samples and core sections break into irregular blocky masses 2 to 10 cm in longest dimension, with irregular to curved, slightly glossy fracture surfaces. In middle Farley outcrops and cores, striations are common on the glossy fracture surfaces (Figure 28). Body fossils are absent from all occurrences, but plant debris is abundant both on outcrops and in cores (Figure 29). Additionally, small tubular structures filled with light brown (5YR 5/6) residues are also common in the middle Farley.

The blocky mudstones of the Island Creek are of a slightly different nature than those found in the middle Farley. The Island Creek blocky mudstones are also massive bedded but have much more consistent coloration. The Island Creek blocky mudstones contain rare body fossils, typically small bivalves. The other main difference is that the blocky mudstones of the Island Creek have no glossy, striated fracture surfaces.

Environmental Interpretation

The blocky mudstones of the middle Farley exhibit features common to ancient soils. Watney *et al.* (1989) indicated diagnostic features used to identify paleosols including: (1) rhizoliths (rootlets), (2) ped surfaces in blocky mudstones, and (3) color mottling or isolated horizons of color. The blocky mudstones of the middle Farley and Island Creek have all of these features.

The blocky or brecciated nature of the mudstones results from the relict ped structure of the soil. Ped surfaces in the middle Farley are recognizable by their irregular to slightly curved surfaces with glossy striated coatings. The slightly glossy, surfaces of the blocky mudstones represent cutans and the striations are slickensides. Slickensides form in clayey soils where peds are repeatedly heaved past one another by swelling and shrinking during episodes of wetting and drying (Retallack, 1990).

The mottled coloration of the middle Farley blocky mudstones is also characteristic of paleosols. Color mottling is typically a result of differential oxidation of iron and redistribution and formation of clay minerals (illuviation) (Watney *et al.*, 1989). Further evidence of paleosol development are the small tubular structures that represent rootlets. Based on these several characteristics common to paleosols, the blocky mudstones of the middle Farley are confidently identified as ancient soil horizons.

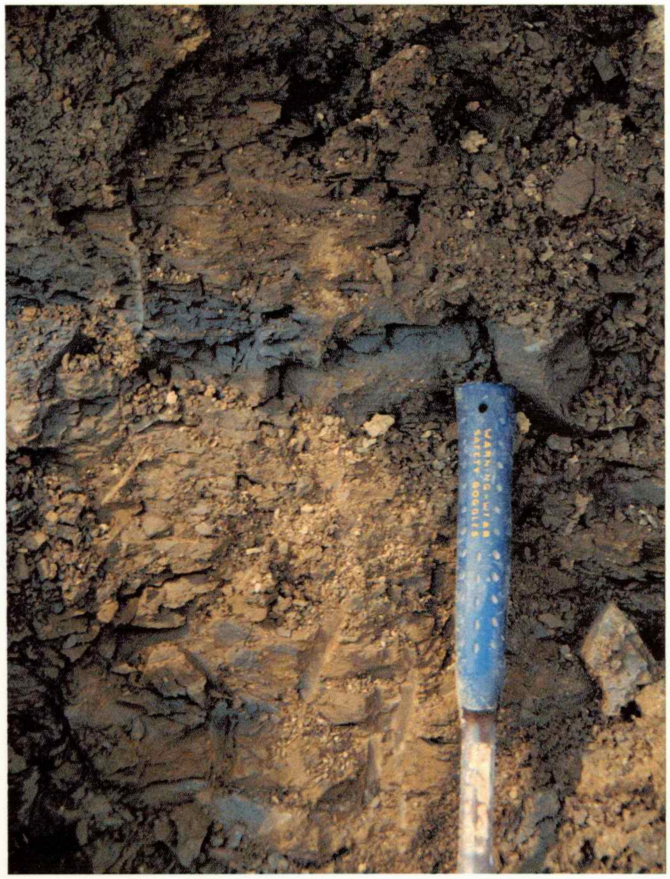

Figure 27. Blocky mudstone in the middle Farley as it appears on weathered outcrop. Note the blocky texture and color variations. (locality MCI)

Figure 28. Detail photograph of ped surface from the blocky mudstone facies. Note the glossy appearance and the striations on the surface. The glossy coating is the soil cutan and the striations are soil slickensides (sample from middle Farley, locality SRS).

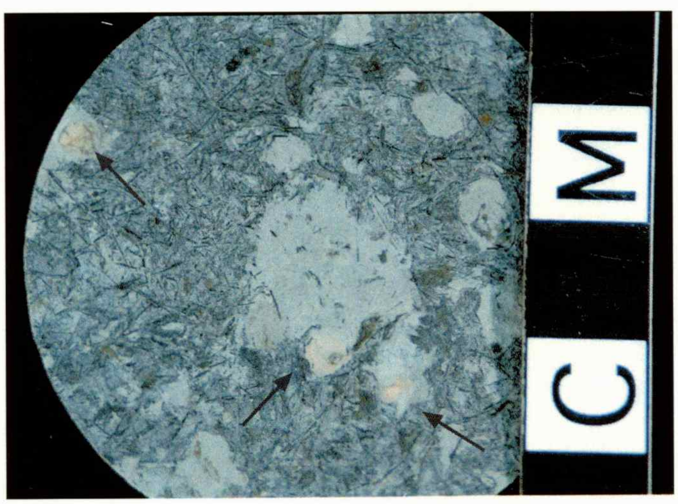

Figure 29. Cross-section of core section with abundant plant material. Plant material (leaf, root and twig fragments) is very abundant in the blocky mudstone facies and is typically well preserved. Also note vertical root tubes visible in the core (arrows) (Core #4-Island Creek).

The lack of paleosol features and the presence of small body fossils indicates a different origin for the blocky mudstones of the Island Creek. The blocky mudstones of the Island Creek are interpreted as prodelta deposits. Prodelta deposits are characteristically fine-grained muddy sediments often containing shell remains and plant and wood debris (Reineck & Singh, 1975). Shepard (1957) described prodeltaic deposits of the modern Mississippi as homogeneous, structureless fine-grained clays and silty clays deposited in water depths greater than about 120 feet.

Stratigraphic Correlations and Sequence-Stratigraphic Interpretations

The stratigraphic correlations discussed below are illustrated in Figures 30 to 34. These figures are cross-sections and a fence diagram that present information gathered from stratigraphic description of outcrops, quarry exposures, and drill cores. The goal of these correlations is to establish a sequence-stratigraphic framework that identifies sequence boundaries that indicate rise and fall of sea level as well as other significant stratigraphic surfaces on a regional scale (e.g., flooding surfaces). The establishment of such a framework in which sea-level history is known allows the examination of other influences on deposition such as depositional topography and distribution of siliciclastics. The following sections present the regional and stratigraphic distribution of lithofacies and uses their interpreted depositonal environments and further detailed observations relevant to their sequence-stratigraphic interpretation to evaluate the controls on regional distribution of lithofacies.

Stratigraphic Datum

The basal bed of the upper Farley (30 to 90 cm thick) contains the only *Osagia*-brachiopod packstone facies found. This bed has consistent lithologic character and

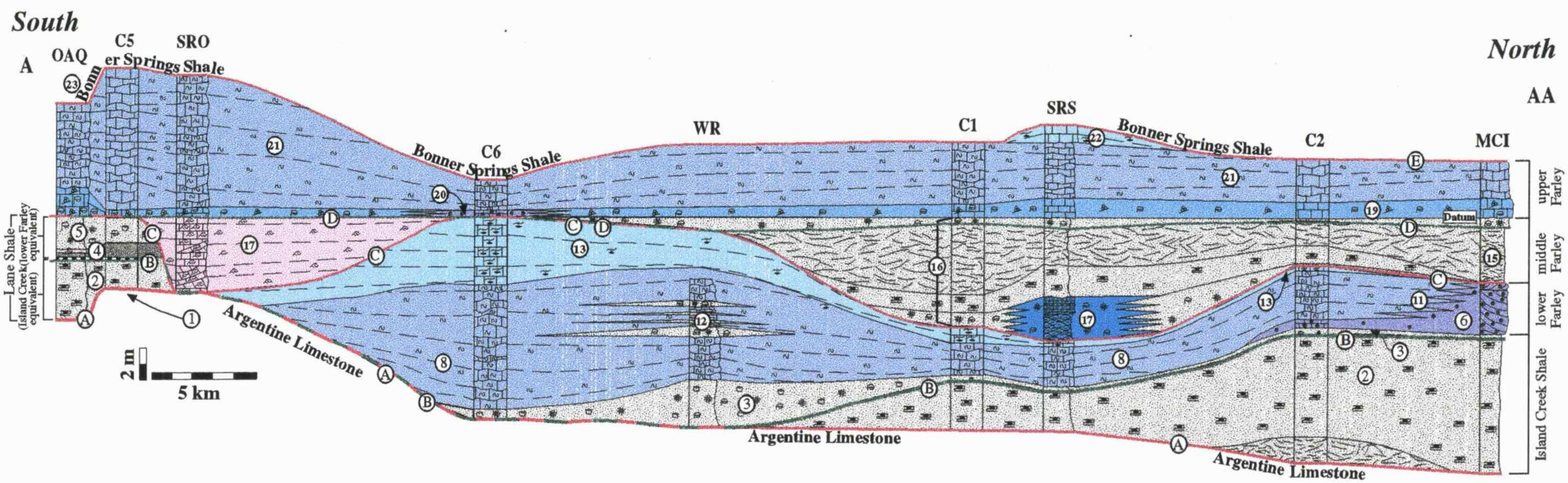

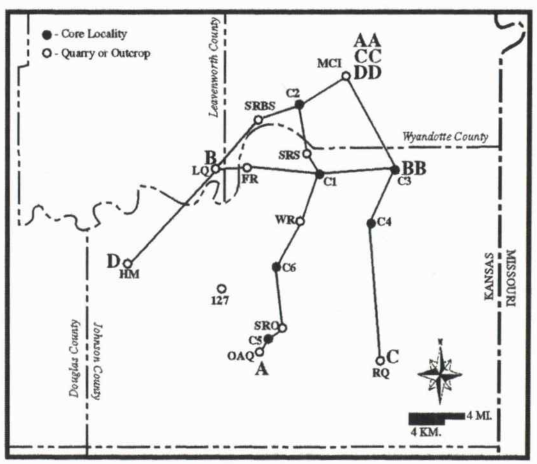

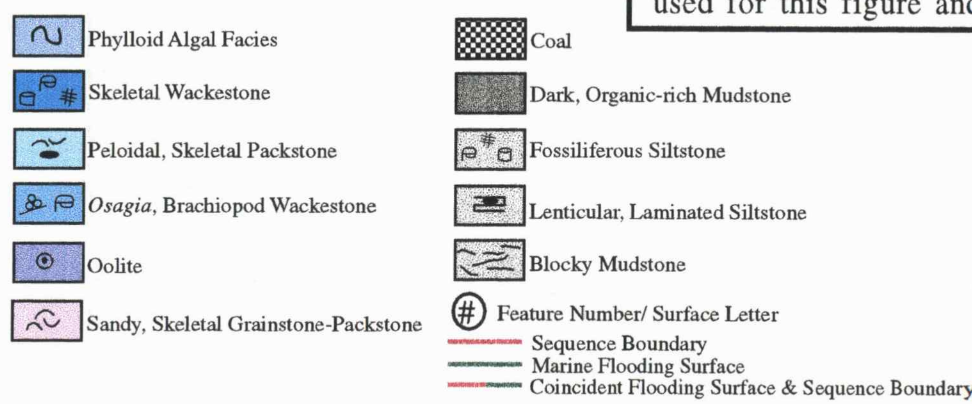

Figure 30. Reconstructed cross-section along line A-AA. Index map shows localities used all stratigraphic reconstructions. Legend outlines lithologic symbols and color codes used for this figure and Figures 31-33.

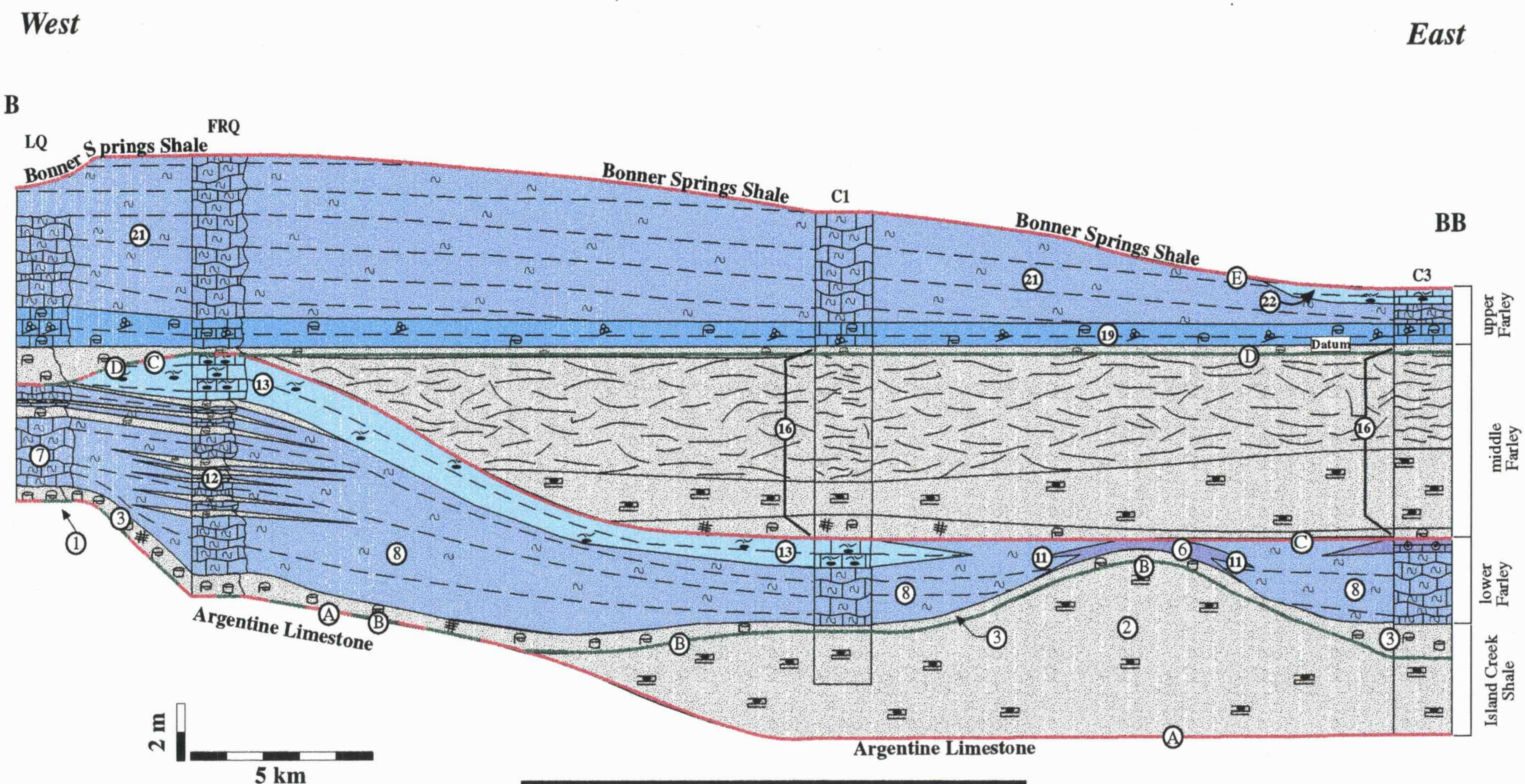

Figure 31. Reconstructed cross-sections along line B-BB. See figure 30 for legend and index map.

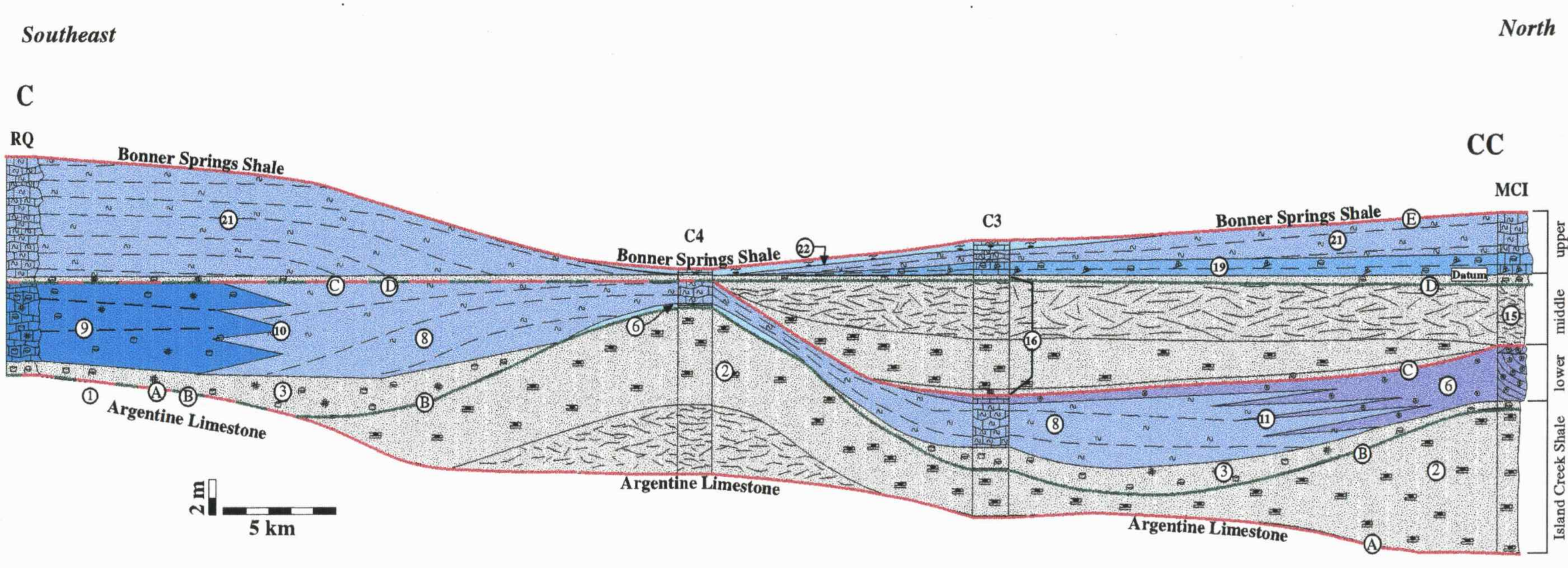

Figure 32. Reconstructed cross-sections along line C-CC. See Figure 30 for index map and legend.

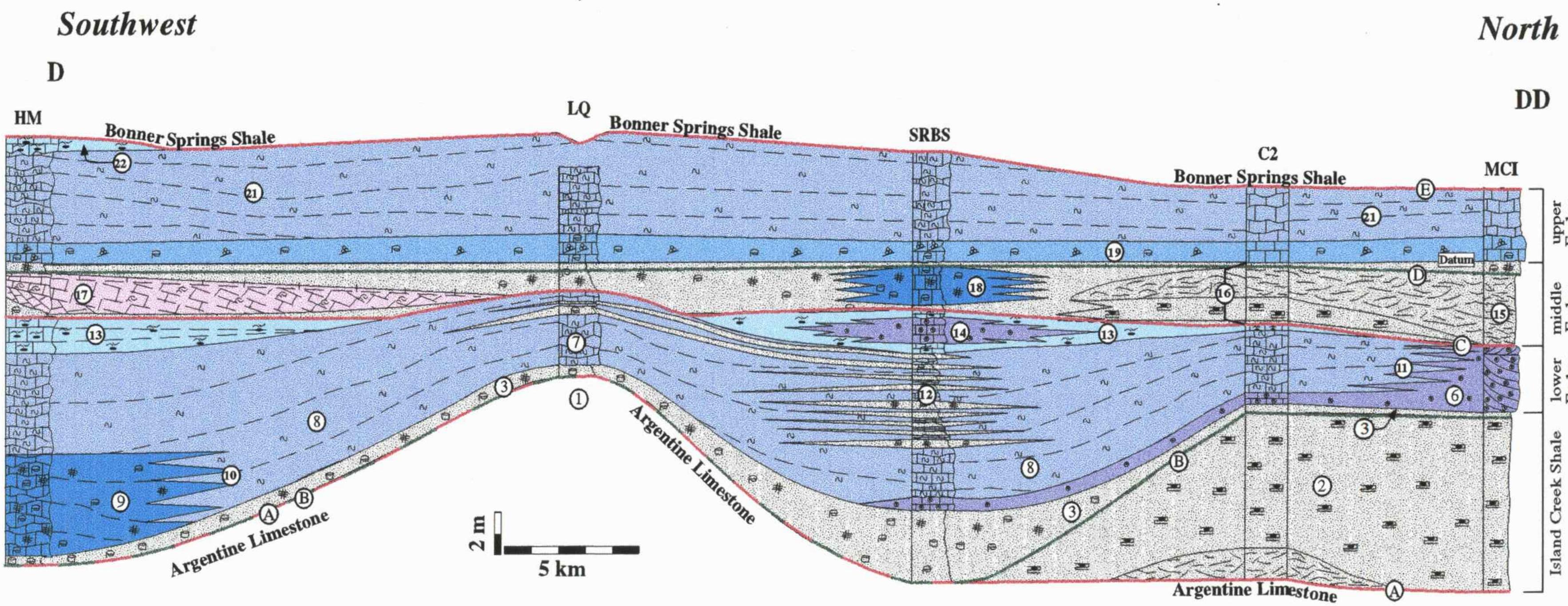

Figure 33. Reconstructed cross-section along line D-DD. See Figure 30 for locality map and legend.

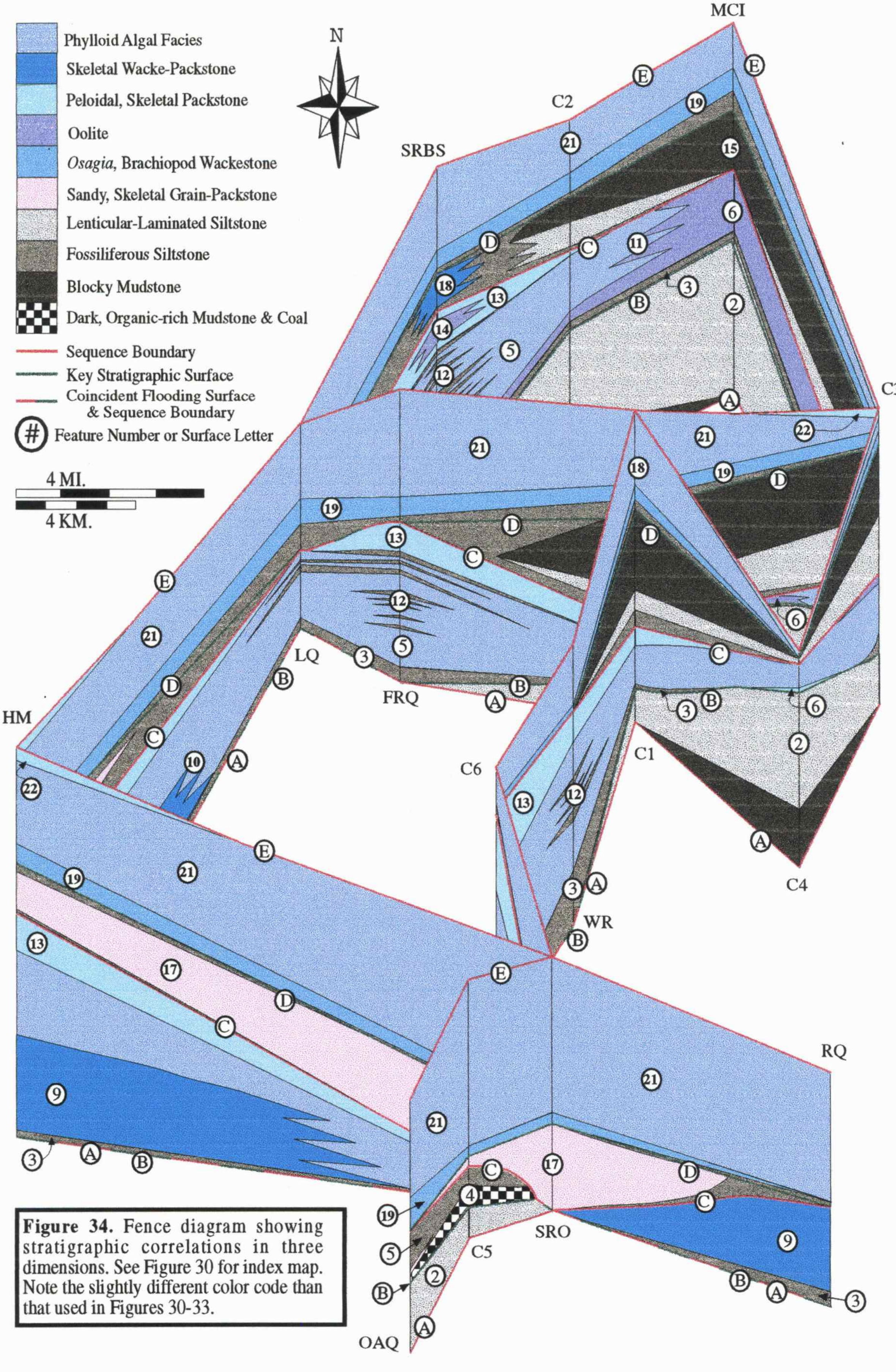

Figure 34. Fence diagram showing stratigraphic correlations in three dimensions. See Figure 30 for index map. Note the slightly different color code than that used in Figures 30-33.

stratigraphic location throughout the field area. The bed is recognized by a zone of whole brachiopods, brachiopod fragments, and other skeletal fragments that are encrusted with *Osagia*. The lithologic consistency of this thin bed suggests a similar environment throughout the area and is interpreted to have been deposited on a relatively flat depositional surface. For these reasons, the basal bed of the upper Farley makes an excellent marker bed and is the datum for the stratigraphic reconstructions (Figures 30 to 33). Use of this datum allows the closest possible reconstruction of actual depositional topography.

Isopach mapping based on data from Crowley (1969) and this study (Figure 3) shows thickened areas of Argentine Limestone in the northeast, northwest, and southeast corners with an additional, slightly thickened area near the center of the field area. These topographic highs in the Argentine are also apparent in the reconstructed cross-sections (Figures 30-33: Feature 1), which further indicates that the basal bed of the upper Farley is a reasonable datum to use for the stratigraphic reconstructions.

The stratigraphic reconstructions offered do not depict exact depositional topography for two main reasons. First, other regional work by Watney *et al.* (1989) suggests that the area may have had a slight south-southwestward dip that cannot be shown in the cross-sections. Second, compaction of shale and silt following deposition can alter thicknesses of a stratigraphic succession by as much as 40-50 percent (Tucker, 1991). These factors provide additional difficulties when attempting to accurately depict depositional topography. The following discussion separates the correlated strata into three stratigraphic intervals with related surfaces and discusses their origin.

Argentine Limestone (Stratigraphic Surface A)

The Argentine Limestone is the carbonate unit located directly under the Lane-Island Creek shales or the Farley Limestone at all localities (Figures 30-33). The

Argentine Limestone has been interpreted as a fully marine unit with such facies as phylloid algal packstones, oolite, and skeletal packstone (Crowley, 1969; Watney *et al.*, 1989; Arvidson, 1990; this study)

Throughout the field area the Argentine Limestone has an irregular surface near its top that has been interpreted as a marine hardground or firmground (Watney *et al.*, 1989). This surface is most prominently developed in the west, center, and south (Localities HM, RQ, WR) where it is overlain by a thin fossiliferous siltstone. These areas received little to no siliciclastic influx, and this surface near the top of the Argentine represents the first significant surface in the sequence-stratigraphic framework of the Lane-Island Creek shales and the Farley Limestone (Figures 30-34: Surface A). This surface appears to be a surface of nondeposition that coincides with the time period between termination of Argentine carbonate deposition and the influx of the siliciclastics of the Lane-Island Creek shales discussed below.

Lane-Island Creek Interval

Directly overlying the Argentine Limestone in the north (localities MCI, C2), east (locality C4), and the south (localities OAQ, C5) are thick siltstones that are somewhat thinner in the east and west-central areas (localities SRS, C1 & C3) (Figures 30-34: Feature 2). These siltstones comprise the Lane-Island Creek shales, and the facies present are dominantly laminated to lenticular bedded siltstones but also include local accumulations of blocky mudstone. As discussed previously, these siltstone facies are interpreted as delta front to prodelta deposits. It is important to consider what controlled the distribution of these deposits.

Isopach mapping of the Lane-Island Creek interval (Figure 4) suggests that the siliciclastics form two separate deltaic units with source in different directions. The Island Creek appears to have has a northern source, whereas the Lane has a southern source. Comparison of isopach maps for the Argentine Limestone and the Lane-Island Creek shales (Figs 2.3 & 2.4) suggest that the distribution of the deltaic siliciclastics was closely controlled by the subtle depositional topography of the Argentine Limestone. There are paleotopographic highs (thicks) in the Argentine Limestone in the northwest and northeast corners of the field area, and the Island Creek appears to fill a channel-shaped depositional low between these two topographic highs. Furthermore, the Island Creek delta thins into and terminates against a topographic high in the Argentine in the southeast corner of the area (Figures 3 & 4). This distribution of siliciclastics suggests that the deltaic deposits of the Island Creek did not form a topographically positive lobe or wedge as suggested by earlier authors (Crowley, 1969; Arvidson, 1990). Instead, these deltaic siliciclastics seemed to have behaved more as valley fills by filling depositonal lows in the underlying limestone.

Distribution of the Lane deltaic sediments in the southern part of the field area also appears to have been controlled by the paleotopography of the Argentine Limestone (Figures 3 & 4). The lower part of the Lane delta extends into the area from the southwest and covers a broad area. This broad distribution could have been because there were fewer topographic restrictions on the underlying Argentine Limestone (Figure 2.4). The same isopach maps (Figures 3 & 4) suggest that the siliciclastics of the Lane-Island Creek deltas in part onlapped highs in the Argentine Limestone.

The presence of deltaic siliciclastics immediately overlying the marine Argentine Limestone is interpreted as the result of a relative fall in sea level. This relative sea-level fall allowed the influx of deltaic siliciclastics from the north (Island Creek) and the south (Lane), which terminated deposition of Argentine carbonates. Interpretation of a relative sea-level fall is supported by the presence of two separate deltaic units that encroached into the area from different directions at the same time. Although the presence of deltaic sediments overlying Argentine carbonates could have resulted from autogenic delta-lobe switching, the presence of two deltas entering the area from different directions at the same time would be unexpected; their migration is more likely the result of a relative sea-level fall. Thus, the boundary separating the underlying Argentine Limestone from the overlying siliciclastics of the Lane-Island Creek shales is interpreted as a sequence boundary (Figures 30 to 34: Surface A).

A lack of evidence of subaerial exposure in the Lane-Island Creek or along the top of the Argentine Limestone indicates that the relative sea-level fall was not extensive enough to expose the upper surface of the Argentine within the study area. It was, however, great enough to allow deltas to enter the area from both the north and south. This increase in siliciclastic input effectively shut down carbonate production. In areas receiving no deltaic siliciclastic influx, a marine hardground developed in the upper portion of the Argentine Limestone.

Upper Island Creek-Lower Farley Interval

The lower Farley interval consists of a variety of siltstone and carbonate facies throughout the field area. The initial deposits of this interval are fossiliferous siltstones that are interpreted as accumulations of marine, prodeltaic sediments. These deposits overlie the deltaic siliciclastics of the Island Creek in the north and occur immediately over the Argentine Limestone in the western, southwestern, and central portions of the area where there are no deltaic siliciclastics (Figures 30 to 34: Feature 3). The fossiliferous siltstones are not present over the deltaic siliciclastics to the south in the area of the Lane delta. Instead, in this area the deposits immediately overlying the deltaic siliciclastics are composed of coal and dark, organic-rich shale with a local accumulation of sandy, skeletal grainstone-packstone (Figures 30, 34: Feature 4).

The fossiliferous siltstones to the north and west are correlated with the coal and dark, organic-rich mudstones and sandy, skeletal grainstone-packstones in the middle portion of the Lane delta to the south because the fossiliferous siltstones and the coal and dark, organic-rich mudstones and grainy skeletal bed all provide evidence of a marine flooding unit. These lithologies are similar to those described for flooding units in other similar Pennsylvanian units by Watney *et al.*, (1989), who stated that lithologies such as thin, fossiliferous siltstones as well as coals capped by invertebrate skeletal lags, are typically flooding units in Pennsylvanian depositional sequences. Furthermore, the widespread, regional extent of these marine lithologies suggests a major flooding event. Thus, the fossiliferous siltstones and the coal and dark, organic-rich mudstone capped by the sandy, skeletal grainstone-packstone are a single flooding unit expressed as different lithologies. Because flooding surfaces are important in interpreting the sequence stratigraphy, the base of this flooding unit is identified as the next key stratigraphic surface (Figures 30 to 34: Surface B).

Based on its lithofacies, the environments represented by the flooding unit have been interpreted as marine (fossiliferous siltstone) or restricted marine (dark, organic-rich mudstone). This switch to more marine facies suggests that siliciclastic sources had become more distal, and waters were more normal marine in salinity. Therefore, the transition from deltaic clastics to marine or restricted marine clastics probably resulted from a relative rise in sea level. In areas that received little to no deltaic influx, the marine flooding surface coincides with surface A, so that surfaces A and B are coincident in places.

Following the relative rise of sea level, carbonate production was established in all areas except the area of the Lane delta in the south, where fossiliferous siltstones continued to accumulate as prodelta deposits of the Lane delta while the lower Farley carbonates were being deposited (Figures 30, 34: Feature 5). Oolites and peloidal, skeletal packstones accumulated in the north and east along topographic highs formed by the thick complex of the Island Creek siliciclastics (Figures 30 to 34: Feature 6). The thickness of the deltaic deposits produced a slight topographic prominence along which elevated energies prevailed due to shallower water depths. Phylloid algal facies are located in lows and directly over topographic highs (Figures 31, 33: Feature 7) in the west, indicating deeper water depths to the west. Such an increase in depth was likely to have been due to original depositional slope which was approximately 0.6 $^{m}/_{km}$ to the west-southwest (Watney et al, 1989).

The greatest accumulations of phylloid-algal limestones in the lower Farley interval are generally located in topographic lows adjacent to topographic prominences on either the Argentine Limestone or the Island Creek delta. (Figures 30 to 33: Feature 8). Therefore, it appears most likely that the phylloid algae of the lower Farley Limestone did not contribute to the construction of depositional topography as suggested by previous authors (Heckel & Cocke, 1969; Harbaugh, 1959, 1960; Arvidson, 1990). Although interpretation of phylloid algae located in depositional lows is contrary to the normal interpretation of topography construction for such facies, it is not new. Matheny and Longman (1996) showed that some of the phylloid-algal facies of the Paradox Basin are concentrated in depositional lows caused by salt solution. Ball *et al.* (1977) suggested that phylloid algae did not construct topography but were instead only a source of sediment that typically collected in depositional lows between deltaic depocenters. The situation in the lower Farley Limestone is likely to have been a combination of these two interpretations. Much of the phylloid algal material is fragmental and apparently not in growth position, which suggests that it may have been transported into the depositional lows. There are, however, also occurrences of phylloid-algal boundstone that may have grown in the lows and not been transported. At this time the exact controls on the distribution of the phylloid algal facies are unknown.

In the southeast and southwest, in areas of deeper water farthest from deltaic siliciclastics, the quiet-water, skeletal wackestone-packstone facies was deposited (Figures 32 to 34: Feature 9). A more open-marine environment, promoted the deposition of the skeletal wackestone-packstone facies, was present in deeper, clear waters distal to the deltas and farther down the regional slope. Up the depositional slope to the north, there was a facies transition to phylloid-algal facies as water shallowed slightly (Figures 32 to 34: Feature 10). Farther to the north, the phylloid-algal facies grades to oolites where the shallowest water occurred (Figures 30, 31, 33, 34: Feature 11).

In one north-northwest to south-southeast trend, the lower Farley limestones are interbedded with marine shales and siliciclastics, becoming more abundant and coarser to the north-northwest (Figures 30-34: Feature 12). This suggests a shifted source of deltaic siliciclastics from the north-northwest with siliciclastics more abundant over underlying topographic lows. This supports the interpretation of Harris (1985) who suggested that the thin accumulations of siltstone in the Farley resulted from periodic influxes from the still active Island Creek delta to the northwest.

This shift in influx of siliciclastics is predictable given filling of the topography on the top of the Argentine Limestone by the Island Creek delta. The suggestion is that the siliciclastics in the lower Farley behaved in a manner similar to those of the Island Creek and preferentially filled depositional lows rather than constructing positive lobes or wedges. Because the valley in which the Island Creek siliciclastics were deposited was full or because sea-level rose above it, deposition of siliciclastics in the lower Farley shifted and found new low areas to fill.

In the western and central portions of the field area the lower Farley is capped by peloidal, skeletal packstone with local accumulations of oolitic, peloidal packstone (Figures 30, 31, 33, 34: Feature 13). These lithofacies indicate slightly elevated energy levels in which currents washed fine carbonate mud. An oolitic, peloidal packstone (locality SRBS) is sandwiched between beds of peloidal skeletal packstone (Figures 33, 34: Feature 14). This oolitic, peloidal packstone contains meniscus cement fabrics and keystone vugs, evidence for subaerial exposure of this facies prior to deposition of the immediately overlying peloidal, skeletal packstone.

The distribution of the peloidal, skeletal packstone facies is problematic. Peloidal, skeletal packstones and oolitic, peloidal packstones are located on and adjacent to topographic prominences in the lower Farley but not on the highest prominences. It is unknown what caused this distribution. One might have expected the highest energies to have been present on the paleotopographic highs and that packstones were generated there. But high energy present over the topographic highs may have swept carbonate sands off the highs into adjacent topographic depressions. Alternatively, currents may have been concentrated in paleotopographic low areas generating packstones in place.

The evidence of subaerial exposure within the deposits at locality SRBS suggests that deposition of the peloidal, skeletal packstones at the top of the lower Farley resulted from a relative fall in sea level. This would explain why the facies is present in the topographically lower areas and not found on the highest highs. If sea level fell, the topographic prominences may have been exposed subaerially and received no carbonate deposition. The presence of marine siltstone directly above these deposits, however, suggests that sea level may have risen again slightly following the deposition of the oolitic, peloidal packstone facies before continuing the drop that formed the sequence boundary located along the top of the lower Farley discussed below. This subtle fluctuation in sea level may help to explain the unusual distribution of peloidal, skeletal packstone facies within the lower Farley, with a minor relative sea-level fall bringing shallow waters and concentrating currents in paleotopographic lows.

Comparison of isopach maps for the lower Farley interval (Figure 35) to those for the Argentine Limestone (Figure 3) and the Lane-Island Creek shales (Figure 4) illustrates that where the Argentine is thin the Lane-Island Creek is thick. Furthermore, where the lower Farley is thickest the Argentine Limestone is thin. Thus, the combined affect of Lane-Island Creek deposition followed by lower Farley Limestone deposition was to greatly reduce, but not completely eliminate, depositional topography. This is contrary to trends outlined by earlier authors (Heckel & Cocke, 1969; Crowley, 1969; Harbaugh, 1959, 1960; Arvidson, 1990) who suggested that thick accumulations of carbonates show a pronounced stacking pattern in which the thickest accumulations of one limestone directly overlie the thickest accumulations of the previous limestone unit thereby perpetuating topography upward in the stratigraphic section.

Top of Lower Farley-Middle Farley Interval

A prominent surface (Figures 30-34: Surface C) separates the lower Farley from the middle Farley. Along this surface, nonmarine blocky mudstones with paleosols directly overlie marine limestones in the north (Figures 30, 32-24: Feature 15) suggesting subaerial exposure and possible erosion. The presence of nonmarine, blocky mudstones immediately over lower Farley limestones indicates a sequence boundary between the two units (Figures 30-34: Surface C). Elsewhere, these blocky mudstones are underlain by fossiliferous siltstones and lenticular, laminated siltstones that sit atop the limestones of the lower Farley (Figures 30-33: Feature 16). Clearly, there must be some complex internal geometries within the siliciclastics of the middle Farley, the structure of which is as yet unknown. The

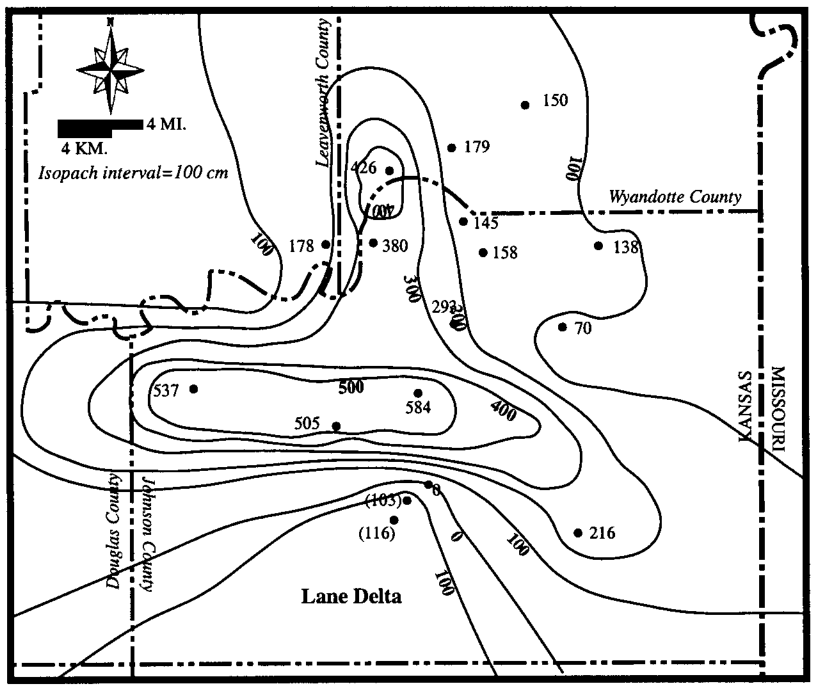

Figure35. Isopach map of lower Farley limestone and equivalent shales to the south in the area of the Lane delta that was still active during deposition of the lower Farley. Note how the lower Farley thickness compliments the underlying Lane-Island Creek thickness variations illustrated in Figure 4. In areas where the Lane-Island Creek is thick, the lower Farley is thin and where the Lane-Island Creek shales are thin, the lower Farley is thick. The lower Farley limestone farther to the south is absent and instead is represented by a portion of the time-equivalent Lane Shale. Data from current study.

evidence for shallowing upward to nonmarine deposits in the middle Farley siliciclastics further supports the interpretation of a relative fall in sea level.

In addition to the siliciclastics discussed above, the middle Farley also contains deposits of sandy, skeletal grainstone and packstone (Figures 30, 33, 34: Feature 17). In the southwest, this facies is cross-bedded and located between beds of siliciclastics (Figures 33, 34: locality HM). This stratigraphic observation supports its correlation to other deposits of the middle Farley. In the south (localities SRO, C5), the sandy, skeletal grainstone-packstone is located in a trough-shaped low between the Lane delta to the south and a topographic high in the lower Farley to the north (Figures 30, 34-36).

This sandy, skeletal, cross-bedded grainstone-packstone lithofacies must have been deposited in a high-energy environment that was influenced by both marine and terrigenous input. The depositional lows into which it was deposited may have resulted from erosional channeling or by deposition in trough-shaped areas between constructional topography. For the southern example, the terrigenous material may represent material eroded from the Lane delta to the south, which perhaps was redeposited in depositional lows where tidal energy was focused. This interpretation of erosion of the Lane delta also is consistent with the absence of the middle Farley interval along the top of the delta. The example from the southwest (locality HM) is somewhat similar to the Pennsylvanian strata at Hamilton Quarry described by Feldman *et al.* (1990) in which a conglomerate was deposited in a system of relatively high-energy barriers and tidal inlets, mainly as part of an estuarine and lagoonal complex. In the Farley, the association of fossiliferous siltstones and cross-bedded facies suggest a similar setting to that of Hamilton Quarry. The example from the south (localities SRO, C5) is similar to that described by Cunningham and Franseen (1992) for a unit possibly equivalent to the Captain Creek Limestone. They suggested that such grainy units were

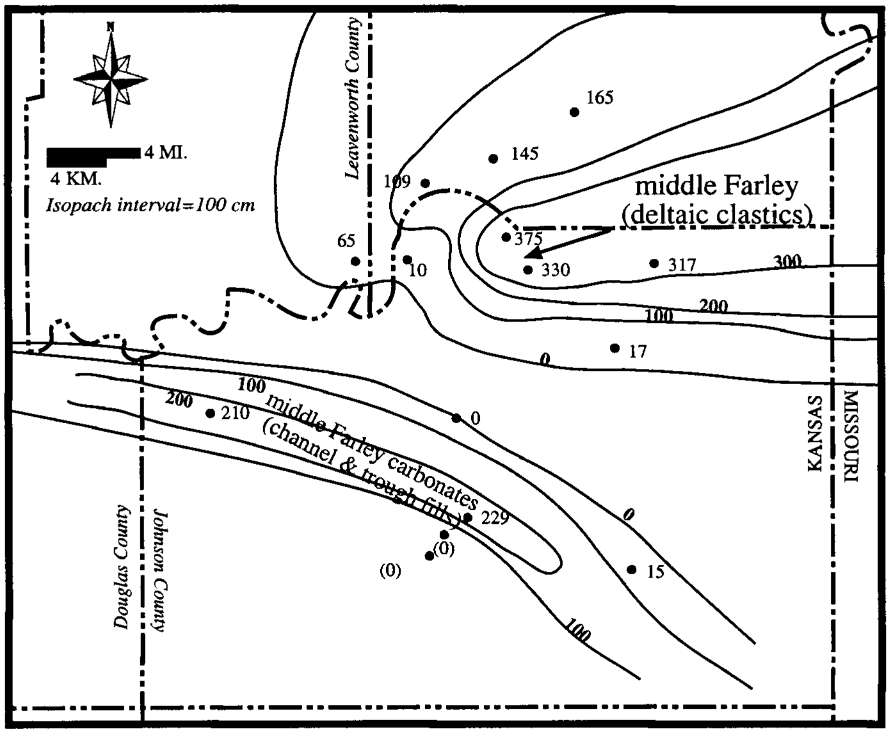

Figure 36. Isopach map showing thickness variations of the middle Farley Shale. The main delta lobe extends into the area from the northeast (arrow). The southern portion of the middle Farley is interpreted to represent a barrier bar and distributary channel system located off the distal end of the delta. Data from current study.

deposited in tidally influenced, topographic lows between algal build-ups where elevated energies resulted from constriction and focusing of tidal energies.

Local accumulations of skeletal wackestone-packstone also occur within the middle Farley at SRS and SRBS (Figures 30, 33, 34: Feature 18). At locality SRS, this facies is highly argillaceous and represents accumulation of argillaceous carbonate as a facies of the middle Farley. This argillaceous carbonate accumulated in what may have been a slight topographic low adjacent to the distal end of middle Farley deltaic deposition. The origin of the skeletal wackestone-packstone at SRBS is more problematic. This accumulation of skeletal wackestone-packstone is not argillaceous and contains only fine, fragmental skeletal material. It is also likely to be a facies of the middle Farley deltaic deposits but is less argillaceous due to a slightly more distal setting. The distribution of these facies are difficult to explain and with only two occurrences in the Farley no obvious control on their distribution is clear.

Isopach mapping for the middle Farley interval indicates that the underlying topography had an impact on the distribution of middle Farley deposits. Judging from the thicknesses, the deltaic siliciclastics of the middle Farley had a northeastern source (Figure 36) and seem to have terminated against the thickened portions of the lower Farley (Figures 35 and 36).

Top of the Middle Farley-Upper Farley Interval

The lithofacies at the top of the middle Farley interval (Figures 30 to 34: Feature 16) suggests that deposition of the upper Farley carbonates was initiated following a relative rise in sea level. This relative sea-level rise is indicated by the thin layer of fossiliferous siltstone that overlies the nonmarine blocky mudstones (Figures 30 to 33: top of Feature 16). This layer represents a marine flooding unit, and the base of this fossiliferous siltstone bed represents the fourth significant surface in the sequence stratigraphic framework (Figure 30-34: Surface D). This siltstone lithofacies was deposited only in parts of the field area closest to the source of middle Farley siliciclastics.

The *Osagia* marker bed (Figures 30 to 34: Feature 19) generally marks the next event of the flooding. This marker bed is found in most of the field area and is recognized by the presence of *Osagia*-brachiopod packstone near the base that grades up to phylloid-algal facies. This widespread consistency of facies indicates that there may have been little to no depositional topography that would have compartmentalized environments and lithofacies as occurred in the lower Farley interval.

There are, however, some places in which the marker bed is missing. One locality (C6) in the center of the field area, from which the distinct marker bed is absent and which contains no middle Farley siliciclastics, provides a potential correlation problem. A thin oolite bed (Figure 30: Feature 20) is present, however, that is correlated with the marker bed. Evidence that this correlation is correct is found to the south at OAQ and the southwest at HM. The marker bed at both of these localities contains abundant ooids that were likely to have been transported from the accumulation of oolite located on a slight topographic high located in the center of the field area (C6). The marker bed is also missing towards the southeast (locality RQ), which is possibly due to deeper water caused by regional dip, which was not conducive to formation of the *Osagia*-brachiopod packstone facies.

The dominant facies of the upper Farley is the phylloid-algal facies, which is present in all localities except one (C4) (Figures 30-34: Feature 21). This facies is consistent in character throughout the area and shows only gradual thickness change (Figures 30 to 34, 37) and less facies variation relative to the deposits of the lower and middle Farley. This relatively gradual thickness variation and lateral consistency in facies may be a result of subdued depositional topography. By this stage of Farley deposition, most depositional topography had been reduced by filling with the deposits of the Lane-Island Creek as well as the lower and middle Farley. Therefore, the upper Farley exhibits much greater consistency in both thickness (Figure 37) and lithofacies (Figures 30 to 34).

Localized accumulations of peloidal, skeletal packstone occur along the top of the upper Farley (Figures 30-34: Feature 22). This lithofacies indicates higher energy was present in some areas near the end of upper Farley deposition. Similar to occurrences of this facies in the lower Farley, the distribution of these peloidal, skeletal packstones in the upper Farley is somewhat enigmatic. Those located in the east (Figure 32: localities C3 & C4) are thin and located between areas of thickened phylloid-algal limestones. Here, even the *Osagia* marker bed is missing, suggesting erosion. It is possible that the peloidal, skeletal packstone was deposited in this area due to higher energy levels that resulted from concentration of currents between thickened accumulations of phylloid algal facies. This higher energy level then resulted in the erosion of some of the underlying facies, such as the *Osagia* marker bed, at C4.

At localities farther to the west (SRS and HM) the peloidal, skeletal packstone facies resembles the upper part of the Argentine Limestone, where it had been interpreted as a possible hardground. This is especially true at locality HM in the southwest, where there is an undulating but razor-sharp contact with the phylloid-algal facies below and where the peloidal facies also has a distinctly reddish color. The peloidal, skeletal packstone facies varies from approximately 20 to 100 cm in thickness in this locality. At locality SRS it is similar in appearance to that at HM but constitutes a single massive bed approximately 1.5 m thick along the top of the upper Farley. This bed is very even in thickness and flat-topped throughout the quarry and contains abundant, large bivalve fossils along the upper surface that suggest that this surface may have been encrusted with bivalves. These occurrences of peloidal, skeletal facies

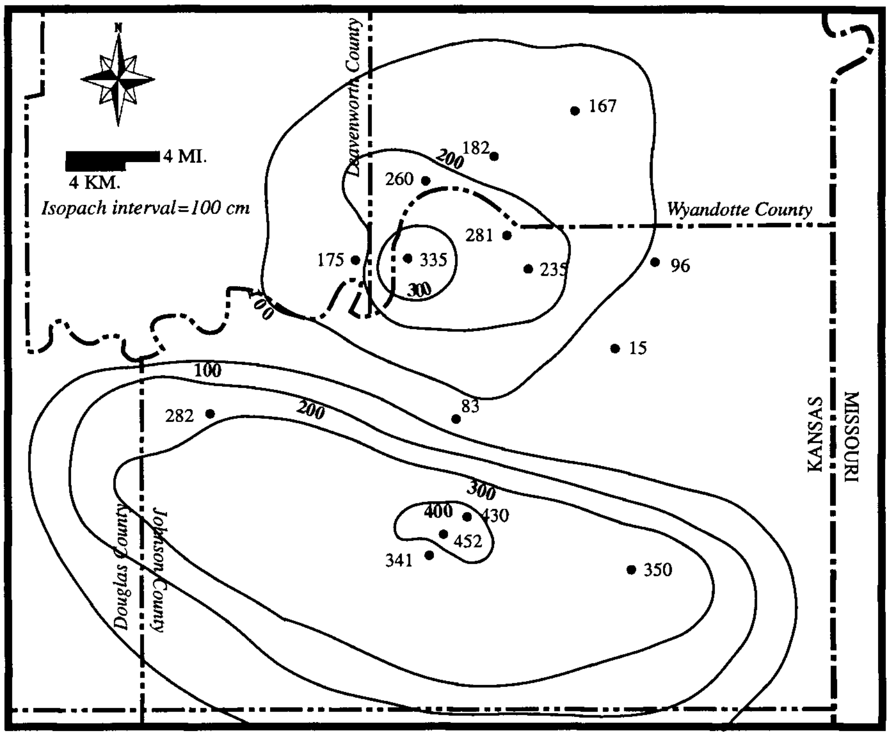

Figure 37. Isopach map showing thickness variation of upper Farley interval. The thickness variations of this interval are more gradual than those found in underlying units (Figs. 3, 4, 35, 36). This is likely due to subdued depositional topography that followed deposition of the Lane-Island Creek and the lower-middle Farley intervals. This subdued topography allowed for more even facies and thickness distribution in the upper Farley.

are likely to have been the result of the development of a hardground along the top of the upper Farley which is missing in surrounding localities due either to nondevelopment or to erosion prior to the deposition of the overlying Bonner Springs Shale. Evidence of Bonner Springs erosion is further discussed below.

Deposition of the Farley Limestone was terminated by the next influx of siliciclastics. The overlying Bonner Springs Shale is a thick sequence of marine and nonmarine siliciclastics that contains evidence of widespread subaerial exposure and erosion (Enos *et al.*, 1989; Watney *et al.*, 1989; Arvidson, 1990; this study). For example, at locality OAQ in the south (Figure 30: Feature 23) the lower part of the Bonner Springs Shale comprises a coarse-grained conglomerate that contains large (centimeter scale) clasts of what appear to be upper Farley phylloid algal facies. Other evidence of erosion previous to deposition of the Bonner Springs Shale is found in the Hunt-Midwest Sunflower quarry (locality HM) to the southwest. In this quarry, the upper Farley could be seen to start to pinch out apparently from erosion prior to deposition of the overlying Bonner Springs Shale. For this reason, the final significant stratigraphic surface in the framework of the Farley Limestone (Figures 30 to 34: Surface E) is drawn as a sequence boundary along the upper surface of the Farley Limestone.

Conclusions

The lateral and vertical variability observed in the Lane-Island Creek Shales and the Farley Limestone is the result of the interaction of fluctuating relative sea level, depositional topography, and the source direction and distribution of siliciclastics. Fluctuating relative sea level acted on a regional scale to cause large-scale changes in deposition such as the influx of deltaic siliciclastics or subaerial exposure of certain units. On a more localized scale, depositional topography had the greatest control on the lateral and vertical distribution of lithofacies by influencing depositional environments.

The presence of two thick deltaic sequences overlying the marine Argentine Limestone indicates a relative fall in sea level between Argentine Limestone deposition and the deltaic Lane-Island Creek shales. Although delta lobe switching could explain the deltaic influxes, the presence of two separate deltas that entered the area from different directions during the same time would be unexpected with delta lobe switching. A lack of evidence of subaerial exposure in the Lane-Island Creek or along the top of the Argentine Limestone indicates that the fall was not extensive enough to expose the upper surface of the Argentine within the study area. The interpretation therefore, is that the upper surface of the Argentine represents the correlative conformity of an unconformity that was likely to have been located further to the north. The relative sea-level fall was, however, great enough to allow deltaic sediments to enter the area from both the north and south.

The lateral distribution of these deltaic sediments was closely controlled by the depositional topography of the underlying Argentine Limestone. The Island Creek deltaic deposits extended into the area from the north through a trough-shaped depositional low between two highs in the Argentine Limestone. In this manner, the Island Creek delta behaved as a valley fill rather than as a traditional delta lobe. The distribution of the southern Lane delta was also controlled by Argentine topography. The Lane shows a broader distribution due to fewer topographic restrictions in the Argentine Limestone to the south. In areas between the two deltas that received no influx of deltaic siliciclastics, a marine hardground developed along the upper surface of the Argentine Limestone.

The presence of a flooding unit and fully marine deposits along the top of the thickened Island Creek delta in the north indicates the termination of deltaic deposition in the Island Creek delta. The change to carbonate deposition could have resulted from a relative rise in sea level or by a delta switch with no accompanying sea-level rise. The presence of a marine, carbonate-rich unit along the top of the Island Creek delta, however, indicates a relative rise in sea level.

Siliciclastic influxes remained somewhat active through lower Farley deposition, however, and its effects are represented by successions of alternating argillaceous phylloid-algal limestones and fossiliferous siltstones at several localities in the northwestern and central portions of the field area. As with the previous Island Creek siliciclastics, these pulses of deltaic siliciclastics were deposited in topographically low areas.

Following the relative sea-level rise, carbonate production was established throughout the northern and central area and depositional topography played a major role in the lateral and vertical distribution of lithofacies. High energy facies such as oolite and peloidal, skeletal packstone accumulated across topographic highs along the thickened Island Creek delta, whereas more quiet-water facies like phylloid algal boundstone and packstone and skeletal wackestone-packstone accumulated in the topographic lows where current energies were weaker.

Near the end of the lower Farley interval, higher energies were present, and as a result peloidal, skeletal packstones and oolitic, peloidal packstones accumulated along the top of the lower Farley in many places. These facies are found over and adjacent to some topographic prominences but are not found over the highest highs. Furthermore, there is evidence for subaerial exposure in the oolitic, peloidal packstones which are immediately overlain by additional marine facies. This relationship suggests that sea-level dropped then rose briefly before continuing to fall again. This could help account for the odd distribution of peloidal, skeletal packstones along the top of the lower Farley.

Lower Farley carbonate deposition was terminated by the influx of middle Farley siliciclastics into the area from the east-northeast. Like the deltaic influx of the Lane-Island Creek, the middle Farley delta influx followed a relative fall in sea level. This fall, however, was great enough to expose much of the delta in the study area and paleosols developed leading to the interpretation of a second sequence boundary. Associated with this deltaic influx was the deposition of the sandy, skeletal grainstone-packstone facies. This facies represents a high-energy environment located in tidally influenced channels or in trough-shaped topographic lows through which current energies were focused.

A second relative rise in sea level is indicated by a second marine flooding unit (fossiliferous siltstone) found along the top of the subaerially exposed middle Farley delta. This flooding unit is overlain by the fully marine upper Farley, which is relatively consistent in thickness and facies throughout the area. This consistency in facies is likely to be due to a relative lack in existing depositional topography. By this point in the deposition of the Farley Limestone, most depositional topography present starting with the Argentine Limestone had been filled with the deposits of the Lane-Island Creek shales as well as the lower and middle Farley limestones.

Finally, carbonate deposition of the Farley Limestone was terminated by a major relative sea-level fall that resulted in the accumulation of the Bonner Springs Shale and widespread exposure, erosion and paleosol development.

The complex distributions of carbonate and siliciclastic lithofacies described in the Lane-Island Creek and Farley Limestone illustrate the profound effect of paleotopography on the rock record. It was shown that carbonate and siliciclastic deposition responds to factors related to energy and accomodation, which in turn are greatly influenced by depositional topography. Siliciclastics are commonly focused into paleotopographic lows of various origins; and, unlike what would be commonly expected, phylloid-algal facies of this interval seem to have a tendency to also fill lows rather than to accumulate on the highs.

References

Arvidson, R.S., 1990, Stratigraphy, carbonate petrology, diagenesis, and trace element cement geochemistry of the Wyandotte limestone (Upper Pennsylvanian), Miami County, Kansas: Unpub. Master's Thesis, University of Iowa, 213 p.

Ball, S.M., Pollard, W.D., and Roberts, J.W., 1977, Importance of phylloid algae in development of depositional topography- reality or myth? *in* Reef and Related Carbonates, Ecology, and Sedimentology: American Association of Petroleum Geologists, Studies in Geology, No. 4, p. 239-259.

Clarkson, E.N.K., 1993, Invertebrate Paleontology and Evolution: London, Chapman & Hall, 434 p.

Crowley, D.J., 1969, Algal-bank complex in the Wyandotte Limestone (Late Pennsylvanian) in Eastern Kansas: Kansas Geological Survey, Bulletin 198, 52 p.

Cunningham, K.J. and Franseen, E.K., 1992, Conglomeratic Limestones of the Upper Pennsylvanian Captain Creek Limestone and their Association with the Lower Sequence Boundary of the Stanton Depositional Sequence, Northwestern Johnson County, Kansas: Kansas Geological Survey Open-file Report 92-51 47 p.

Enos, P., Herman, D., Watney, L., and Franseen, E., 1989, Stop 4: I-70/I-435 Interchange: Bonner Springs Shale and Plattsburg Limestone *in* Watney, W.L., French, J.A., and Franseen, E.K., eds. Sequence stratigraphic interpretations and modeling of cyclothems in the Upper Pennsylvanian (Missourian), Lansing and Kansas City groups in eastern Kansas: Guidebook of the Kansas Geological Society, 41st Annual Fieldtrip, p. 115-125.

Feldman, H.R., Franseen, E.K., Fahr, T.R. and Maples, C.G., 1990, Geology and Sedimentology of the Hamilton Lagerstatte *in* Cunningham, C.R., and Maples C.G., eds., 1990 Society of Vertebrate Paleontology Upper Paleozoic of Eastern Kansas Excursion Guidebook, Kansas Geological Survey Open-file Report 90-24, p. 37-41.

Ginsburg, R.N., 1960, Ancient analogues of recent stromatolites: International Geological Congress, Report of the 21st Session Norden, Pt. 22, p. 26-35.

Golubic, S., Perkins, R.D., and Lukas, K.J., 1975, Boring microorganisms and microborings in carbonate substrates *in* Fray, R.W., ed., The Study of Trace Fossils: A Synthesis of Principles, Problems, and Procedures in Ichnology: New York, Springer-Verlag, p. 229-259.

Harbaugh, J.W., 1959, Marine bank development in Plattsburg limestone (Pennsylvanian), Neodesha-Fredonia area, Kansas: Kansas Geological Survey, Bulletin 134, p. 289-331.

———1960, Petrology of marine bank limestones of Lansing group (Pennsylvanian), Southeast Kansas: Kansas Geological Survey, Bulletin 142, p. 189-234.

———1964, Significance of marine banks in Southeastern Kansas in interpreting cyclic Pennsylvanian sediments: Kansas Geological Survey, Bulletin 169, p. 199-203.

Harris, J., 1985, Stop 2: Intersection of K-7 and K-32 Highways, East Edge of Bonner Springs: Wyandotte Limestone Stratigraphy *in* Watney, W.L., Kaesler, R.L., and Newell, K.D., eds., Recent Interpretations of Late Paleozoic Cyclothems: Proceedings of the 3rd Annual Meeting and Field Conference, Mid-Continent Section, Society of Economic Paleontologists and Mineralogists, p. 31-33.

Harris, P.M., 1984, Cores from a Modern Carbonate Sand Body: The Joulters Ooid Shoal, Great Bahama Bank *in* Harris, P.M. ed., Carbonate Sands—A Core Workshop: Society of Economic Paleontologists and Mineralogists Core Workshop No. 5, p. 429-464.

Heckel, P.H., 1972, Recognition of ancient shallow marine environments *in* Rigby, J.K., and Hamblin, W.K., eds., Recognition of Ancient Sedimentary Environments: Society of Economic Paleontologists and Mineralogists, Special Publication, No. 16, p. 226-286.

———1977, Origin of phosphatic black shale facies in Pennsylvanian cyclothems of Mid-continent North America: American Association of Petroleum Geologists, Bulletin, v. 61, p. 1045-1068.

Heckel, P.H., and Cocke, J.M., 1969, Phylloid algal-mound complexes in outcropping Upper Pennsylvanian rocks of Mid-continent: American Association of Petroleum Geologists, Bulletin 53, p. 1058-1074.

Hinds, H., and Greene, F.C., 1915, The stratigraphy of the Pennsylvanian series in Missouri: Missouri Bureau of Geology and Mines, v. 13, 2nd series, p. 75-102.

Johnson, J. H., 1946, Lime-secreting algae from the Pennsylvanian and Permian of Kansas: Geological Society of America, Bulletin, v. 57, p. 1087-1120.

———1963, Pennsylvanian and Permian algae: Quarterly of the Colorado School of Mines, v. 58, no. 3, 211 p.

Konishi, K., and Wray, J.L., 1961, *Eugonophyllum*, a new Pennsylvanian and Permian algal genus: Journal of Paleontology, v. 35, p. 659-666.

Matheny, J. Paul, Longman, M. W., 1996, Power Desert Creek Reservoirs in the Paradox Basin: examples of phylloid algae filling depositonal lows related to salt dissolution *in* Longman, M.W., & Sonnenfeld, M.D., eds., Paleozoic Systems of the Rocky Mountain Regions. Rocky Mountain Section, Society of Economic Paleontologists and Mineralogists, p. 267-282.

Moore, D.G., and Scruton, P.C., 1957, Minor internal structures of some recent unconsolidated sediments: American Association of Petroleum Geologists, Bulletin, v. 41, p. 2723-2751.

Moore, R.C., 1932, A reclassification of the Pennsylvanian system in the northern Mid-Continent region, Guidebook, Sixth Annual Field Conference: Kansas Geological Society, p. 79-97.

———1935, Stratigraphic classification of the Pennsylvanian rocks of Kansas: Kansas Geological Survey, Bulletin 22, p. 116-124.

———1949, Divisions of the Pennsylvanian system in Kansas: Kansas Geological Survey, Bulletin 83, 203 p.

Newell, N., 1935, Geology of Johnson and Miami counties, Kansas: Kansas Geological Survey, Bulletin 21, p. 55-181.

Ramsbottom, W.H.C., 1978, Carboniferous *in* McKerrow, W.S., ed., The Ecology of Fossils: Massachusetts, The MIT Press, p. 146-183.

Reineck, H.E., and Singh, I.B., 1975, Depositional Sedimentary Environments: New York, Springer-Verlag, 439 p.

———1980, Depositional Sedimentary Environments—With Reference to Terrigenous Clastics: Springer-Verlag, Berlin, 439 p.

Retallack, G.C., 1990, Soils of the Past: Boston, Unwin Hyman, 520 p.

Shepard, F.P., 1964, Criteria in modern sediments useful in recognizing ancient sedimentary environments *in* VanStraaten, L.M.J.U., ed., Developments in Sedimentology: Deltaic and Shallow Marine Deposits, v. 1, p. 1-25.

Tedesco, L.P., and Wanless, H.R., 1989, Role of burrow excavation and infilling in creating the preserved depositional fabric of Pennsylvanian phylloid mounds of southeastern Kansas *in* Watney, W.L., French, J.A., and Franseen, E.K., eds. Sequence stratigraphic interpretations and modeling of cyclothems in the Upper Pennsylvanian (Missourian), Lansing and Kansas City groups in eastern Kansas: Guidebook of the Kansas Geological Society, 41st Annual Fieldtrip, p. 115-125.

Tucker, M.E., 1991, Sedimentary Petrology: An Introduction to the Origin of Sedimentary Rocks: Oxford, Blackwell Scientific Publications, 260 p.

Tsien, H.H, 1985, Algal-bacterial origin of micrites in mud mounds *in* Toomey, D.F., and Nitecki, M.H. eds., Paleoalgology, contemporary research and applications: Springer-Verlag, Berlin, p. 290-296.

Watney, W.L., French, J. A., Franseen, E.K., 1989, Sequence stratigraphic interpretations and modeling of cyclothems in the Upper Pennsylvanian (Missourian), Lansing and Kansas City groups in eastern Kansas: Guidebook of the Kansas Geological Society, 41st Annual Fieldtrip, 211 p.

Watney, W.L., and Heckel, P.H., 1994, Revision of the stratigraphic nomenclature and classification of the Marmaton, Pleasanton, and Kansas City groups in Kansas: Kansas Geological Survey, Open File Report 94-34, p. 1-18.

Wilson, J.L., 1970, Depositional facies across carbonate shelf margins: Gulf Coast Association of Geological Societies Transactions, v. 20, p. 229-233.

Wilson, J.L., and Jordan, C., 1983, Middle Shelf Environment, *in* Scholle, P.A., Bebout, D.G., and Moore, C.H., eds., Carbonate Depositional Environments: American Association of Petroleum Geologists, Memoir 33, p. 297-344.

Wray, J.L., 1964, *Archeolithophyllum*, an abundant calcareous alga in limestones of the Lansing Group (Pennsylvanian), southeastern Kansas: Kansas Geological Survey, Bulletin 170, pt. 1, 13 p.

-------- 1968, Late Paleozoic phylloid algal limestones in the United States: 23rd International Geological Congressional Report, Prague.